Chinese Journal of Natural Medicines

Natural resources, chemical synthesis, chemo–bio transformations, metabolism, pharmacology, toxicology, and the underlying mechanisms of curdione

Suyan Liu, Jiayin Han, Yushi Zhang, Dewen Liu, Jintang Cheng, Chen Pan, Aihua Liang

Citation: Suyan Liu, Jiayin Han, Yushi Zhang, Dewen Liu, Jintang Cheng, Chen Pan, Aihua Liang, Natural resources, chemical synthesis, chemo–bio transformations, metabolism, pharmacology, toxicology, and the underlying mechanisms of curdione, Chinese Journal of Natural Medicines, 2026, 24(3), 257–269. doi: 10.1016/S1875–5364(26)61101–6.

View online: https://doi.org/10.1016/S1875–5364(26)61101–6

Chinese Journal of Natural Medicines 24 (2026) 257-269

Contents lists available at ScienceDirect

Chinese Journal of Natural Medicines

journal homepage: www.cjnmcpu.com/

Review

Natural resources, chemical synthesis, chemo-bio transformations, metabolism, pharmacology, toxicology, and the underlying mechanisms of curdione

Suyan Liu, Jiayin Han, Yushi Zhang, Dewen Liu, Jintang Cheng, Chen Pan, Aihua Liang*

State Key Laboratory for Quality Ensurance and Sustainable Use of Dao-di Herbs, Institute of Chinese Materia Medica, China Academy of Chinese Medical Sciences, Beijing 100700, China

ARTICLE INFO

Article history:
Received 26 March 2025
Revised 17 June 2025
Accepted 20 June 2025
Available online 20 March 2026

Keywords:
Curdione
Source
Metabolism
Bioactivity
Toxicity
Mechanism

ABSTRACT

Curcuma is a traditional Chinese medicine that has been utilized for centuries in the treatment of various diseases. Terpenoids, particularly monoterpenes and sesquiterpenes, constitute the primary bioactive components of the essential oil derived from *Curcuma* species. Among these, curdione—one of the key active constituents—has been identified in 25 *Curcuma* species, with the highest concentration reported in the rhizome essential oil of *Curcuma trichosantha* Gagnep. Curdione can also be synthesized through chemical methods, and its regio- and stereo-selectivity can be further optimized *via* chemo-bio transformations. This compound demonstrates significant therapeutic potential, including anticancer, antithrombotic, anti-inflammatory, anti-viral, anti-fungal, anti-diabetic, and multi-organ protective properties. Despite these promising biological activities, its clinical application is hindered by poor water solubility and potential toxicity. This review summarizes current knowledge on the natural sources, chemical synthesis, chemo-bio transformations, metabolism, pharmacokinetics, pharmacological effects, potential toxicities, and molecular mechanisms of curdione. Furthermore, perspectives on future drug development are discussed with the aim of promoting the clinical translation of this promising natural compound.

1. Introduction

Natural products and their derivatives represent rich sources of bioactive compounds for drug discovery and development [1]. Herbal medicines have been used for thousands of years worldwide to treat various diseases. *Curcuma*, an important genus in the family *Zingiberaceae*, includes several species—such as *Curcuma longa* and *C. caesia*—that possess significant edible, medicinal, and economic value. *Curcuma* is traditionally used to remove blood stasis, promote *qi* circulation, stimulate menstrual flow, and relieve pain. It exhibits anti-inflammatory, hepatoprotective, and immunomodulatory activities and has been employed clinically for over a thousand years. Zedoary turmeric oil (ZTO), extracted from *Curcuma*, is commonly used in clinical practice to treat gynecological disorders, viral lower respiratory tract infections, viral enteritis, influenza, endometrial cancer, ovarian cancer, and other conditions [2–8]. Additionally, ZTO demonstrates anti-fungal activity against phytopathogens such as *Phytophthora capsica* and *Aspergillus flavus* [9, 10].

Terpenoids, particularly monoterpenes and sesquiterpenes, are the primary constituents and active ingredients of *Curcuma* essential oil [11]. Sesquiterpenes have demonstrated promising anticancer effects against colon, breast, gastric, liver, and other cancer cell lines [12–17]. Moreover, certain sesquiterpenes—including curcumol, germacrone, and *β*-elemene—have shown potential in overcoming chemotherapy resistance [18–20]. Curdione, a sesquiterpene abundant in ZTO, varies in content depending on the *Curcuma* species [21, 22]. Extensive studies have revealed that curdione possesses diverse pharmacological activities, including antithrombotic, anti-inflammatory, anticancer, anti-viral, and multi-organ protective effects. However, there was no comprehensive review summarizing research on curdione currently. To address this gap, this paper reviews studies on the natural resources, chemical synthesis, chemo-bio transformations, metabolism, pharmacokinetics, pharmacological activities, and potential toxicities of curdione, aiming to provide a theoretical foundation for future investigations. Furthermore, challenges in clinical application and prospective research directions to overcome existing limitations are discussed.

2. Natural resources of curdione

Curcuma, belonging to the Zingiberaceae family, comprises approximately 110 species distributed across South and Southeast Asia. These plants are widely utilized in Bengal, China, Sri Lanka, Indonesia, Peru, Australia, and the West Indies [23]. Curdione is broadly distributed in the essential oil of *Curcuma* species. To date, it has been identified in the rhizomes and leaves of 25 *Curcuma* species. The content of curdione varies significantly among different species. As shown in Table 1, relatively high levels of curdione are found in the essential oils of *C. aeruginosa* [24], *C. amada* [25], *C. aromatica* [26, 27], *C. cochinchinensis* [28], *C. harmandii* [29], *C. kwangsiensis* [30], *C. leucorhiza* [31], *C. trichosantha* [32], *C. wenyujin* [30], and *C. zedoary* [33, 34]. Notably, the rhizome essential oils of *C. aromatica* and *C. trichosantha* contain particularly high concentrations—reaching 43.96% and 47.40%, respectively.

* Corresponding author.
E-mail address: ahliang@icmm.ac.cn(A. Liang)

https://doi.org/10.1016/S1875-5364(26)61101-6

The content of curdione also differs across plant parts within the same species. For example, in *C. cochinchinensis*, the curdione content in leaf, small rhizome, large rhizome, and root essential oils was reported as 33.9%, 9.8%, 8.4%, and 2.5%, respectively [28]. Environmental and climatic variations across different geographic regions significantly influence plant growth and the biosynthesis of active medicinal constituents. These factors contribute to notable regional differences in curdione content. For example, essential oils extracted from *C. angustifolia* collected in Jagdalpur and Travancore districts in India contained 0.8% and 8.4% curdione, respectively [40]. In addition to geographical influences, the choice of extraction and separation methods markedly affects curdione yield. One study found that the acetate extract of *C. mangga* rhizomes contained 0.98 $mg \cdot g^{-1}$ of curdione, approximately double the concentration found in chloroform extracts [46]. Moreover, different extraction techniques can significantly alter both the chemical composition and the quantified concentration of curdione. Zhang et al. compared essential oil profiles of C. wenyujin obtained using various extraction approaches and reported relative curdione contents of 13.04% (ultrasound-assisted ethyl acetate extraction), 15.59% (supercritical CO_2 fluid extraction), and 13.56% (steam distillation) [11].

3. Chemical synthesis of curdione

Chemical synthesis remains a traditional approach in drug development. Curdione was first isolated from *C. zedoaria*, and its chemical structure was initially described in 1966 [48]. Neocurdione, an isomer of curdione, is also a naturally occurring compound. Zhao et al. achieved the total synthesis of (−)-curdione

Table 1 The natural resources of cudione and its relative contents.

No.	Curcuma species	Geographical location	Parts	Contents (mg/g or relative content)	References
1	*C. aeruginosa*	Jogorogo village, Ngawi, East Java, Indonesia	Rhizome	-	35
		Phu Thuy village, Gia Lam district, Hanoi, Vietnam	Rhizome	-	36
		Tawangmangu, Central Java, Indonesia.	Essential oil of rhizomes	23.34%	24
		Kerala, India	Essential oil of leaves	1.40%	37
2	*C. albiflora*	Sabaragamuwa, Sri Lanka	Essential oil	2.83%	38
		Kitulgala, Sri Lanka	Essential oil	2.83%	39
3	*C. cf. amada*	Bueng Kan Province, Thailand	Essential oil of rhizomes	16.47%	25
4	*C. angustifolia*	Jagdalpur, India; Travancore, India	Essential oil of rhizomes	0.8%; 8.4%	40
5	*C. aromatica*	Fukuyama, Hiroshima, Japan; Motobu, Okinawa, Japan	Essential oil of rhizomes	43.96%; 32.20%	26
		Thrissur, India	Essential oil of leaves	15.31%	27
6	*C. cochinchinensis*	Vietnam	Essential oil of leaves, small rhizomes, large rhizomes, and roots	33.9%, 9.8%, 8.4%, 2.5%	28
7	*C. comosa*	Nakhon Si Thammarat, Thailand	Rhizomes	0.006%	41
8	*C. elata*	Sawangdaendin district, Sakon Nakhon province, Thailand	Rhizomes	-	42
9	*C. haritha*	Kerala, India	Essential oil of rhizomes	6.90%	43
10	*C. harmandii*	Cao Bang province, Vietnam	Essential oil of leaves, stems, flowers, rhizomes, and roots	36.8%, 25.3%, 27%, 1.9%, 2.2%	29
11	*C. inodora*	Perak, Malaysia	Essential oil of rhizomes	7.50%	44
12	*C. kwangsiensis* var *nanlingensis*	Panyu District, Guangzhou, China	Essential oil of rhizomes	1.66 ± 0.25	30
	C. kwangsiensis	Panyu District, Guangzhou, China	Essential oil of rhizomes	11.12 ± 0.06	30
13	*C. latifolia*	Nakhon Pathom province, Thailand	Rhizomes	0.0807	45
14	*C. leucorhiza*	Wangoo area (Bishnupur District) of Manipur, India	Essential oil of rhizomes and leaves	19.1%, 19.5%	31
15	*C. longa*	Panyu District, Guangzhou, China	Essential oil of rhizomes	0.75 ± 0.02	30
16	*C. mangga*	Yogyakarta, Central Java, Indonesia	Chloroform and acetate extract of rhizomes	0.43, 0.98	46
17	*C. nankunshanensis*	Panyu District, Guangzhou, China	Essential oil of rhizomes	6.16 ± 2.04	30
18	*C. phaeocaulis*	Panyu District, Guangzhou, China	Essential oil of rhizomes	0.30 ± 0.01	30
19	*C. rubescens*	Panyu District, Guangzhou, China	Essential oil of rhizomes	0.25 ± 0.08	30
20	*C. sichuanensis*	Panyu District, Guangzhou, China	Essential oil of rhizomes	0.92 ± 0.10	30
21	*C. singularis*	So Pai commune, KBang district, Gia Lai province, Vietnam	Essential oil of rhizomes	0.72%	47
22	*C. trichosantha*	Vietnam	Essential oil of rhizomes	47.40%	32
23	*C. wenyujin*	Panyu District, Guangzhou, China	Essential oil of rhizomes	13.79 ± 2.01	30
24	*C. zedoaroides*	Dong Hy District, Thai Nguyen Province, Vietnam	Essential oil of rhizomes	27.45%	33
25	*C. zedoaria*	Ruian, China	Essential oil of rhizomes	19.57%	34

Note: "-" detected, but not quantified.

through a sequence involving selective hydrogenation, bromination with *N*-bromosuccinimide (NBS), hydrolysis, hydrogenation, and protection *via* ethoxy ether, starting from (−)-carvone [49]. Curdione is thermally unstable due to the lack of rigidity in its macrocyclodecenedione structure [50]. Studies indicate that curdione readily undergoes tautomerization under heating conditions to form curcumol, with higher temperatures leading to increased conversion yields [51–52].

4. Chemo-bio transformation of curdione

Selective modifications can significantly enhance a compound's stability, pharmacological activity, and safety profile. However, challenges in organic synthesis persist, particularly regarding amines, *N*-heterocycles, unprotected polar groups, site-selective functionalization, and stereoselectivity [53]. Bio-transformation offers an efficient strategy for generating structurally complex and diverse compounds from natural precursors. (4*S*,7*S*)-curdione has been transformed by *Aspergillus niger* (*A. niger*) and *Mucor polymorphosporus* (*M. polymorphosporus*). Seven metabolites were obtained from (4*S*,7*S*)-curdione (**1a**) using *A. niger* AS 3.739: 3α-OH-(4*S*,7*S*)-curdione (**2a**), 2β-OH-(4*S*,7*S*)-curdione (**3a**), (1*S*,4*S*,5*R*,7*S*)-curcumalactone (**4a**), 3α-OH-(1*S*,4*S*,5*R*,7*S*)-curcumalactone (**5a**), 2β-OH-(1*S*,4*S*,5*R*,7*S*)-curcumalactone (**6a**), (10*S*)-9,10-di-OH-curcumalactone (**7**) and (10*R*)-9,10-di-OH-curcumalactone (**8**) (Fig. 1). Notably, *A. niger* AS 3.739 enabled stereoselective hydroxylation of curdione, yielding **2a** as the major metabolite and **3a** in lower yield [54]. Microbial biotransformation of curdione by *M. polymorphosporus* produced five germacrane-type sesquiterpene alcohols: **3a**, **2a**, 1α,10β-epoxy-11-hydroxycurdione (**9**), (2*S*)-2α,11-di-OH-(4*S*,7*S*)-curdione (**10**) and 11,15-di-OH-(4*S*,7*S*)-curdione (**11**) [55]. Qin et al. synthesized (4*R*,7*R*)-curdione (**1b**), the enantiomer of **1a**, using neocurdione as a starting material through reduction, isomerization, and oxidation. Subsequent incubation of **1b** with *A. niger*, followed by acid-catalyzed reactions, yielded the corresponding enantiomers of **2a**, **3a**, **4a**, **5a**, and **6a**, namely 3β-OH-(4*R*,7*R*)-curdione (**2b**), 2α-OH-(4*R*,7*R*)-curdione (**3b**), (1*R*,4*R*,5*S*,7*R*)-curcumalactone (**4b**), 3β-OH-(1*R*,4*R*,5*S*,7*R*)-curcumalactone (**5b**), and 2α-OH-(1*R*,4*R*,5*S*,7*R*)-curcumalactone (**6b**) [56]. These chemo-bio transformative products have expanded the structural diversity of known sesquiterpenoids.

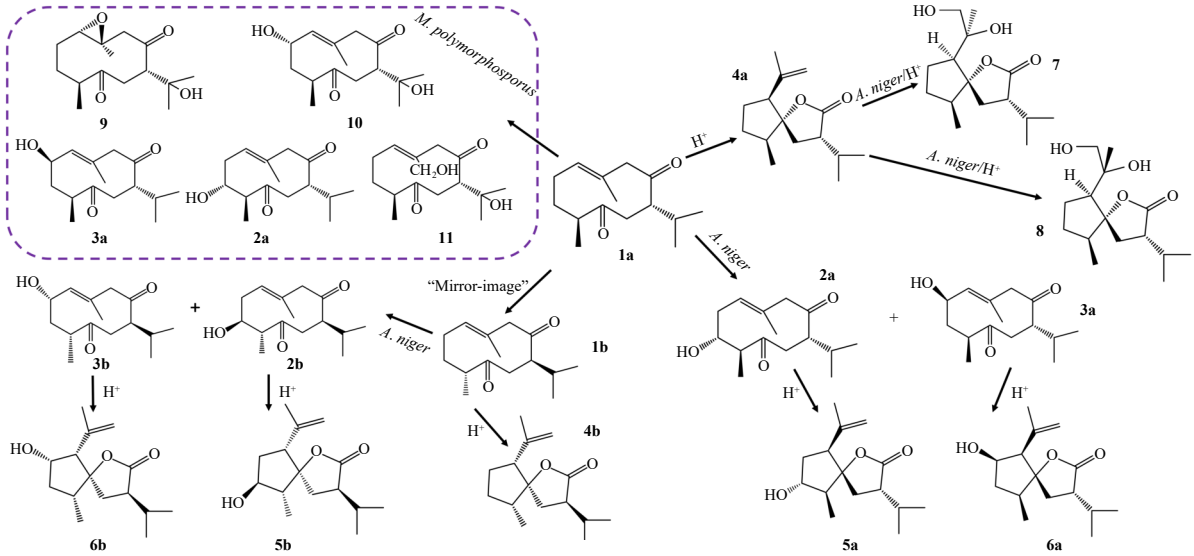

Fig. 1 Chemo-bio transformations of curdione by *A. niger* and *M. polymorphosporus*. Regio- and stereo-selective metabolites of curdione are obtained.

5. Metabolism and pharmacokinetics

5.1. Metabolism

The *in vivo* metabolites of curdione in rats were characterized using UHPLC-Q-exactive Orbitrap mass spectrometry. Following oral administration, curdione underwent extensive metabolism, including oxidation, glucuronidation, and conjugation with ethyl, methyl-sulfinyl, cysteine, and vitamin C moieties. A total of 76 metabolites—63 phase I and 13 phase II—were detected in rat biological samples after administration of 150 mg·kg^{-1} curdione. Among these, 23 metabolites were present in the brain, heart, liver, spleen, lungs, kidneys, stomach, small intestine, and large intestine. Metabolites such as 3-hydroxycurdione, curdione + 2O-2H, curdione + 3O-2H, curdione + O + GluA, (1,10)-epoxy-curdione, and curdione + cysteine were detected in more than three organs and are considered to contribute to the *in vivo* biological activities of curdione [57].

5.2. Pharmacokinetics

You et al. reported that curdione exhibited low intestinal absorption in a rat *in situ* single-pass perfusion model, attributed to its poor water solubility. No significant differences were observed among dosage groups or intestinal regions, suggesting passive diffusion without a specific absorption window [58]. Pharmacokinetic analysis revealed that after a single oral dose of Curcumae Rhizoma essential oil (10 mg·kg^{-1}) in Wistar rats, curdione reached a maximum plasma concentration (c_{max}) of 2420.04 ng·mL^{-1}, with a time to peak concentration (t_{max}) of 1.17 h and an elimination half-life ($t_{1/2}$) of 7.14 h, indicating rapid absorption and moderate elimination [59]. In another study, curdione showed moderate absorption, with a t_{max} of 3.0 h in Sprague-Dawley rats following administration of Curcumae Rhizoma extract (14.17 g·kg^{-1}). A double absorption peak was observed, potentially resulting from enterohepatic recirculation and metabolic interconversion [60]. Such pharmacokinetic variations may arise from differences in rat strain, extraction methods, sample handling, and potential drug-drug interactions (DDIs) within the extracts.

Administration route also influences curdione's pharmacokinetic profile. Peng et al. compared serum pharmacokinetics after intravenous and vaginal administration of ZTO (10.0 mg·kg^{-1}) in rabbits, reporting t_{max} values of 0.083 h and 0.75 h,

respectively. The corresponding c_{max} values were 330.26 ng·mL^{-1} and 46.31 ng·mL^{-1}, while $t_{1/2}$ values were 3.11 h and 5.41 h, respectively. Intravenous administration resulted in rapid absorption and elimination [61]. Rapid absorption enables faster achievement of c_{max}, facilitating prompt therapeutic action, which is beneficial for symptom relief. Conversely, the sharp rise in curdione concentration may increase the risk of adverse reactions. Additionally, fast elimination suggests that dosing frequency or amount may need adjustment in clinical settings to maintain stable plasma concentrations and sustained efficacy.

6. Pharmacological activities of curdione

6.1. Anticancer activity

Curdione exhibits anticancer activity against various solid tumors, including breast cancer, ovarian cancer, cervical cancer, kidney cancer, bladder cancer, and colorectal cancer (CRC) (Table 2). Key mechanisms include inhibition of proliferation, tumor metastasis, and angiogenesis, as well as induction of ferroptosis (Fig. 2).

Table 2 Molecular targets and mechanisms of curdione in different cancers.

Type of cancer	Cell line/Animals	Treatment conditions	IC_{50}	Molecular targets	Mechanisms	References
Breast cancer	MDA-MB-231	125–2000 μmol·L^{-1}	1607 μmol·L^{-1} (24 h) 1401 μmol·L^{-1} (48 h)	Bax↑, Bcl-2↓, Caspase-9↑, cleaved Caspase-9↑, cleaved Caspase-3↑, p53↑, p21↑	G_1 cell cycle arrest, Apoptosis	62
	MCF-7; xenograft nude mouse of breast tumor	50–200 μg·mL^{-1}; injection, 50,100,150 mg·kg^{-1}	125.632 μg·mL^{-1} (72 h)	Bax↑, Bcl-2↓, Caspase-9↑, cleaved Caspase-3↑	Apoptosis	68
	HCC1937	12.5–400 μmol·L^{-1}	> 400 μmol·L^{-1} (24 h) 363.1 μmol·L^{-1} (48 h)	p-ERK↓, p-JNK↓, p-Akt↓, MMP-2↓, MMP-9↓,	Inhibition of cell migration and invasion	84
	MDA-MB-468	0–80 μmol·L^{-1}; Combined with DTX	151.712 μmol·L^{-1} (24 h) curdione 40 μmol·L^{-1} + DTX 1 μg·mL^{-1}	p38↑, Erk↓, NF-κB↓, Akt↓, p21↑, p27↑, Bcl-2↓, Bax↑, Bak↑, apaf-1↑, Cytochrome C↑, Caspase 3↑	ROS production and apoptosis	76
Liver cancer	HepG2	5.9–94.4 mg·L^{-1}	~ 50 mg·L^{-1} (24 h) ~ 30 mg·L^{-1} (48 h) ~ 25 mg·L^{-1} (72 h)	–	G_2/M cell cycle arrest	65
Cervical cancer	HeLa	12.5, 25, 50 μmol·L^{-1}	> 50 μmol·L^{-1} (24 h)	-	Apoptosis inhibition of cell proliferation and invasion	85
Renal cancer	ACHN	12.5, 50, 200 mg·L^{-1}	-	p-PI3K↓, p-Akt↓, Bcl-2↓, p53↑, caspase-3↑, Bax↑	Apoptosis, inhibition of proliferation	75
Uterine leiomyosarcoma	SK-UT-1, SK-LMS-1; SK-UT-1 Xenograft Tumor Model	0.1–500 μmol·L^{-1}; 100, 200 mg·kg^{-1}·d^{-1}, i.p. for 21 days	327.0 μmol·L^{-1} (24 h) 334.3 μmol·L^{-1} (24 h)	P21↑, CyclinB1↑, Cdc2↓; cleaved Caspase-3↑, cleaved Caspase-6↑, cleaved Caspase-9↑; LC3↑, Beclin-1↑, p62↓, IDO1↓	G_2/M cell cycle arrest, apoptosis, and autophagy	64
Bladder cancer	5637, BIU87; Xenograft Tumors	5, 10, 20, 40 μmol·L^{-1}; combined with GEM	Close to 20 μmol·L^{-1} and 10 μmol·L^{-1} (72 h); Curdione (20 μmol·L^{-1}) + GEM (8 μmol·L^{-1})	CA2↓	Inhibition of proliferation and migration	87
Colorectal cancer	CT26, SW480; CT26 xenograft mice	12.5, 25, 50 μmol·L^{-1}; 50, 100, 200 mg·kg^{-1}	> 50 μmol·L^{-1}	METTL14↑, YTHDF2↑, SLC7A11↓, SLC3A2↓, HOXA13↓, GPX 4↓	Ferroptosis	12

Note: (↑) up-regulated; (↓) down-regulated. DTX, docetaxel; GEM, gemcitabine. i.p., intraperitoneal injection.

6.1.1. Inhibition of proliferation

6.1.1.1 Cell cycle arrest

The complete cell cycle consists of G_1, S, G_2, and M phases. Some cells exit into the quiescent G_0 phase and re-enter the cycle upon stimulation by growth factors. Cyclins and their partner cyclin-dependent kinases (CDKs) tightly regulate the cell cycle. Curdione (250, 500, 1000 μmol·L^{-1}) induces G_1 phase arrest in malondialdehyde (MDA)-MB-231 cells by upregulating p53 and p21 proteins [62]. P53, a key cell cycle regulator, can indirectly induce cell cycle arrest *via* the p53-p21-DREAM-E2F/CHR pathway (p53-DREAM pathway) [63]. Curdione also induces G_2/M phase arrest in uterine leiomyosarcoma (uLMS) and HepG2 cells. At concentrations of 25, 50, and 100 μmol·L^{-1}, curdione up-regulates the checkpoint proteins p21 and cyclin B1 while downregulating Cdc2, leading to concentration-dependent G_2/M arrest in uLMS cells [64, 65]. Different cancer cell lines exhibit distinct cell cycle characteristics due to complex gene regulation networks. Additionally, culture conditions and treatment protocols influence the phase of arrest observed [66, 67]. These factors likely explain the differential cell cycle arrest induced by curdione across various cancer cell lines.

6.1.1.2 Apoptosis

Apoptosis is a programmed form of cell death characterized by distinct morphological changes and enzyme-dependent biochemical processes. Caspases, including caspase-3, -6, and -9, are central mediators. Curdione inhibits the proliferation of MDA-MB-231 cells by promoting apoptosis, modulating the expression of apoptosis-related proteins such as B-cell lymphoma-2 (Bcl-2), Bcl-2-associated X protein (Bax), caspase-9, cleaved caspase-9, and cleaved caspase-3 *in vitro* [62]. Furthermore, curdione demonstrates anticancer efficacy *in vivo*. In a xenograft nude mouse model of breast cancer, average tumor weight decreased from 386 ± 34 mg in controls to 332 ± 12 mg ($P < 0.05$), 279 ± 24 mg ($P < 0.05$), and 154 ± 10 mg ($P < 0.01$) following intraperitoneal injection of 50, 100, and 150 mg·kg^{-1} curdione, respectively. Increased expressions of cleaved caspase-3, caspase-9, and Bax, along with decreased Bcl-2 levels, support the role of apoptosis in curdione-mediated tumor suppression. Moreover, the use of a caspase-3 inhibitor confirmed that curdione induces apoptosis in breast cancer cells [68].

Indoleamine-2,3-dioxygenase-1 (IDO1) catalyzes the rate-limiting step in the conversion of tryptophan (Trp) to kynurenine (Kyn) and exerts immunoregulatory effects in cancer therapy [69]. IDO1 also promotes proliferation and progression in various cancers, and its inhibition enhances cancer cell apoptosis [70–72]. Wei et al. demonstrated that curdione inhibits uLMS cell proliferation *in vitro* and suppresses tumor growth in a SK-UT-1 xenograft mouse model *in vivo*. Further investigation revealed that curdione induces apoptosis *via* downregulation of IDO1 and upregulation of cleaved caspases -3, -6, and -9 [64].

Hyperactivation of the phosphatidylinositol 3-kinase (PI3K)/RAC-alpha serine/threonine-protein kinase (Akt) pathway is closely linked to cancer development, making its inhibi-

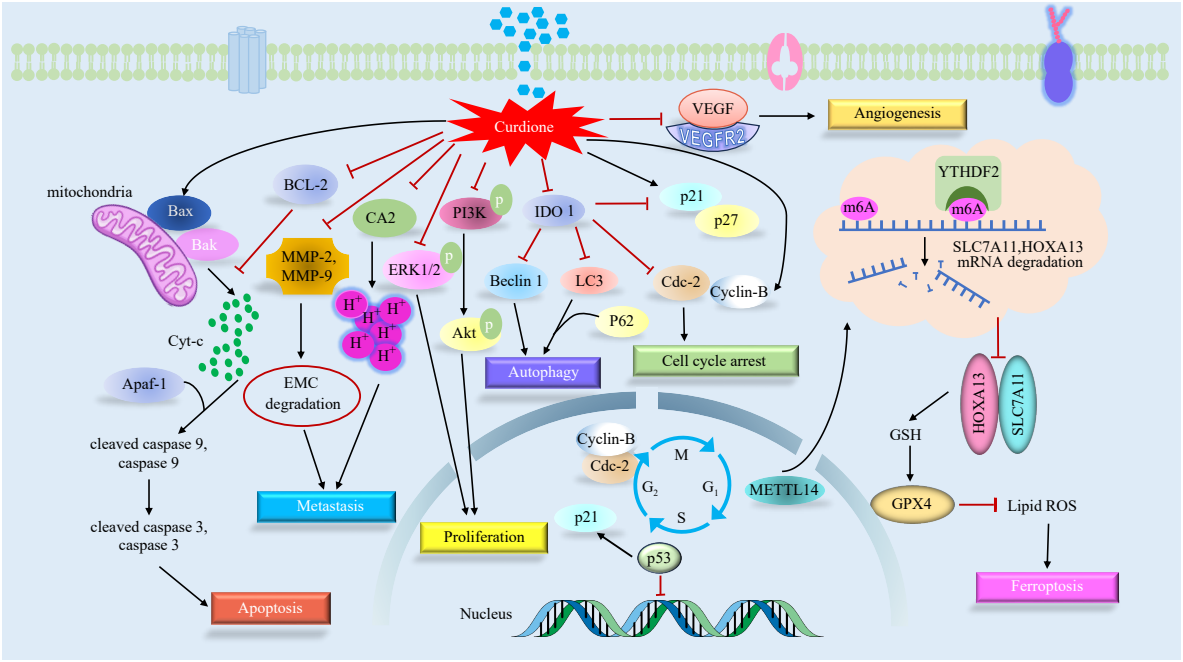

Fig. 2 Anticancer mechanisms of curdione. Inhibition of proliferation, cell invasion, migration, angiogenesis, induction of cell cycle arrest, and activation of apoptosis, ferroptosis are involved.

tion a viable therapeutic strategy [73, 74]. Curdione reduces expression of p-PI3K, p-Akt, and Bcl-2 while increasing caspase-3 and Bax levels in human renal carcinoma ACHN cells, indicating that it induces apoptosis by suppressing the PI3K/Akt signaling pathway [75]. Additionally, curdione enhances the chemotherapeutic effect of docetaxel (DTX) on MDA-MB-468 cells by triggering reactive oxygen species (ROS)-mediated apoptosis through the MAPKs and PI3K/Akt pathways [76].

6.1.2. Activation of autophagy

Autophagy is a self-degradative process that maintains intracellular homeostasis and cell viability by clearing protein aggregates and damaged organelles [77]. However, excessive autophagy often leads to cell death and disease progression [78]. In cancer, autophagy plays a dual role—suppressing tumor initiation while supporting established tumor survival. Despite this complexity, autophagy remains a therapeutic target [79]. Curdione (25, 50, 100 $\mu mol \cdot L^{-1}$) induces autophagy in SK-UT-1 and SK-LMS-1 cells in a dose-dependent manner by upregulating light chain 3 (LC3) and Beclin-1 and downregulating p62 [64].

6.1.3. Inhibition of migration, invasion, and metastasis

Metastasis is the primary cause of cancer-related mortality, involving the spread of malignant cells from the primary tumor site to distant organs. This complex, multistep process requires coordinated regulation of cellular protrusion, chemotaxis, invasion, and contractility to enable directed migration [80]. A key step in metastasis is the degradation of the extracellular matrix (ECM), facilitated by matrix metalloproteinases (MMPs), particularly MMP-2 and MMP-9, which are implicated in various signaling pathways associated with tumor invasion and progression [81–83]. Curdione has been shown to inhibit the invasive potential of cancer cells in a dose- and time-dependent manner. In HeLa and HCC1937 cells, curdione significantly suppresses adhesion, motility, and invasion at concentrations of 12.5, 25, and 50 $\mu mol \cdot L^{-1}$ following 24- or 48-hour treatments. These inhibitory effects are accompanied by downregulation of phosphorylated extracellular signal-regulated kinase (ERK), c-Jun *N*-terminal kinase (JNK), and Akt, as well as reduced expressions of MMP-2 and MMP-9, indicating interference with key signaling pathways involved in cell invasion [84, 85].

Additionally, carbonic anhydrase 2 (CA2), which is overexpressed in invasive urothelial carcinoma (UC) in rats and muscle-invasive bladder cancer (MIBC) in humans, has been identified as a potential marker of tumor invasiveness [86]. Curdione enhances the anti-cancer efficacy of gemcitabine (GEM) *in vitro* by further inhibiting bladder cancer cell proliferation, clonogenic potential, and migratory ability. *In vivo*, curdione significantly reduces xenograft tumor growth, likely through modulation of CA2 expression and function [87].

6.1.4. Activation of ferroptosis

Ferroptosis is a regulated, iron-dependent form of cell death characterized by the accumulation of lipid peroxides and oxidative damage to cellular membranes [88]. Emerging evidence suggests that ferroptosis plays a pivotal role in tumor suppression and in overcoming resistance to conventional therapies [89, 90]. Glutathione peroxidase 4 (GPX4) is a key negative regulator of ferroptosis, relying on intracellular glutathione (GSH) to detoxify lipid hydroperoxides and maintain redox homeostasis [91, 92]. The cystine/glutamate antiporter system Xc^-, particularly its component solute carrier family 7 member 11 (SLC7A11), is essential for sustaining GSH synthesis by facilitating cystine uptake. Recent studies have identified a regulatory mechanism involving methyltransferase-like 14 (METTL14), which mediates N6-methyladenosine (m6A) modification of *SLC7A11* mRNA. This modification promotes mRNA degradation *via* recognition and binding by the m6A reader protein *YTH N6-methyladenosine* RNA binding protein F2 (YTHDF2) [93]. In a study by Wang et al., curdione was shown to inhibit the viability of CT26 colorectal cancer cells *in vitro* by reducing intracellular GSH levels while increasing MDA and ferrous ion concentrations—hallmarks of ferroptosis. Mechanistically, curdione treatment led to the upregulation of *METTL14* and *YTHDF2* and concurrent downregulation of *SLC7A11*, *SLC3A2*, *HOXA13*, and *GPX4*. These molecular alterations were also confirmed *in vivo*, supporting the hypothesis that curdione induces ferroptosis through activation of the m6A–METTL14–YTHDF2–SLC7A11 axis [12].

6.1.5. Inhibition of angiogenesis

Vascular endothelial growth factor (VEGF) is a key mediator

of angiogenesis, enhancing vascular permeability and promoting endothelial cell migration [94]. Overexpression of VEGF contributes significantly to tumor angiogenesis and accelerates the onset, proliferation, and metastasis of liver cancer [95, 96]. Silencing or inhibiting VEGF expression effectively suppresses hepatocellular carcinoma growth, migration, and invasion [97]. Curdione inhibits the proliferative activity of human hepatic sinusoidal endothelial cells (HHSECs) in the HepG2 tumor microenvironment. Incubation with curdione (1 and 2 μg·L^{-1}) significantly reduced mRNA and protein expression of VEGF ($P < 0.01$) and VEGFR2 ($P < 0.01$) [98].

6.2. Anti-thrombus

P-selectin is a glycoprotein expressed on activated platelets and endothelial cells. Upon platelet activation, P-selectin translocates rapidly from intracellular granules to the cell surface, facilitating platelet aggregation *via* fibrinogen and GPIIb/IIIa interactions. Platelet P-selectin expression determines aggregate size and stability [99]. Curdione enters platelets *via* intracellular uptake both *in vitro* and *in vivo* [100–102]. It also inhibits carrageenan-induced tail thrombosis in mice in a dose-dependent manner at 50, 100, and 200 mg·kg^{-1}. The inhibitory potency of curdione against agonist-induced platelet aggregation follows the order: PAF > thrombin > AA > ADP. At 30 and 60 mg·kg^{-1}, curdione significantly reduced ADP-induced platelet aggregation in rats ($P < 0.05$, $P < 0.01$). Further studies showed that curdione lowers plasma P-selectin levels and exerts significant anti-thrombotic effects in thrombosis models. Enhanced NO production, elevated cyclic adenosine monophosphate (cAMP) levels, and inhibition of intracellular Ca^{2+} mobilization collectively augment its anti-thrombotic activity [103, 104].

Integrins, heterodimeric transmembrane receptors including *β1* and *β3* families, play pivotal roles in platelet adhesion and aggregation [105–107]. Talin is essential for integrin activation during hemostasis and thrombosis [108, 109]. Vinculin, a talin-binding protein, promotes integrin-mediated adhesion [110]. Beyond maintaining the discoid morphology of resting platelets, *α*- and *β*-tubulin isoforms mediate morphological changes following activation [111-112]. Curdione modulates vinculin and Talin 1 expression *via β1*-tubulin, thereby affecting integrin signaling and inhibiting platelet activation [113-114]. Fang et al. demonstrated that curdione also suppresses platelet aggregation by regulating the adenosine 5'-monophosphate-activated protein kinase (AMPK)-vinculin/talin-integrin αIIbβ3 signaling pathway [115].

Hemodynamic parameters such as whole blood viscosity (WBV) and shear rate (SR) are associated with thrombosis risk. Elevated WBV predicts high thrombotic risk in cardiovascular patients [116, 117]. High share rate (SR) gradients promote thrombosis in a von Willebrand factor (vWF)-dependent manner [118, 119]. Curdione improves blood circulation and alleviates blood stasis by reducing WBV, plasma viscosity, high shear stress (HSR), and low shear stress (LSR) in adrenaline- and ice water-induced blood stasis rat models at doses of 30–120 mg·kg^{-1}. However, curdione exhibited only mild thrombolytic activity at a high concentration of 0.235 g·L^{-1} *in vitro* [120], suggesting that higher concentrations are required for anti-thrombotic effects. Whether long-term, high-dose administration leads to adverse effects warrants further systematic investigation.

6.3. Anti-inflammatory and analgesic

Tan et al. reported that curdione significantly inhibited xylene-induced ear edema in mice at 200 and 400 mg·kg^{-1} ($P < 0.05$, $P < 0.01$) and carrageenan-induced paw edema at 140 and 280 mg·kg^{-1} ($P < 0.05$, $P < 0.01$). Additionally, curdione (100, 200, 400 mg·kg^{-1}) reduced acetic acid-induced writhing responses ($P < 0.01$) and significantly increased the pain threshold in the hot plate test at 400 mg·kg^{-1} ($P < 0.05$, $P < 0.01$) [121].

Curdione exhibits pronounced anti-inflammatory effects both *in vitro* and *in vivo*. Its anti-inflammatory activity is associated with reduced oxidative stress, suppression of nuclear factor *κ*B (NF-*κ*B) signaling activation, and downregulation of proinflammatory cytokines. Shi et al. used a partial hepatectomy model in aged mice to evaluate curdione's anti-inflammatory effects. Administration of curdione (60 and 120 mg·kg^{-1}) for 8 days significantly increased hippocampal levels of superoxide dismutase (SOD), catalase (CAT), and glutathione peroxidase (GSH-Px) ($P < 0.05$) and reduced MDA concentration ($P < 0.05$). Furthermore, postoperative elevations in NF-*κ*B, interleukin-1β (IL-1β), IL-6, and tumor necrosis factor-α (TNF-α) were markedly suppressed ($P < 0.05$) [122].

Overexpression of prostaglandins (PGs) and cyclooxygenase-2 (COX-2) due to biosynthesis is closely linked to inflammatory and carcinogenic processes [123, 124]. Curdione inhibited PGE_2 production in lipopolysaccharide (LPS)-stimulated RAW 264.7 macrophages in a concentration-dependent manner (half maximal inhibitory concentration, IC_{50} 1.1 μmol·L^{-1}) and reduced COX-2 mRNA expression [125].

Toll-like receptors (TLRs), located on cell membranes and in endosomes, recognize conserved molecular patterns and initiate macrophage activation and polarization. M1-polarized macrophages produce proinflammatory cytokines and express cluster of differentiation 86 (CD86) as a marker [126]. Curdione treatment alleviated clinical symptoms in DSS-induced colitis mice and reduced inflammation. At 30 mg·kg^{-1}, curdione significantly downregulated colonic mRNA expression of *Tnf-α*, *Il-6* ($P < 0.001$), *Il-1β* ($P < 0.05$), and *Inos* ($P < 0.001$), while upregulating the anti-inflammatory cytokine *Il-10* ($P < 0.05$). At 60 and 120 mg·kg^{-1}, curdione significantly inhibited *Il-6* and *Inos* mRNA expression ($P < 0.01$). *In vitro* studies further showed that curdione suppressed expression of *Cd86*, *Tnf-α*, *Tlr2*, *Il-6*, and *Il-1β* in THP-1-derived macrophages, suggesting it may modulate Tlr2 signaling to inhibit M1 polarization and mitigate colitis-associated inflammation [127].

6.4. Cardioprotection

Curdione reduces ROS accumulation and prevents mitochondrial dysfunction induced by doxorubicin (DOX) or isoproterenol (ISO). It attenuates increases in serum creatine kinase-MB isoenzyme (CK-MB) and lactate dehydrogenase (LDH) and inhibits apoptosis by modulating Bcl-2 and Bax expression. Additionally, curdione decreases phosphorylation of ERK1/2 and JNK and activates the nuclear factor erythroid 2-related factor 2 (Nrf2)/heme oxygenase-1 (HO-1) and Nrf2/SOD1/HO-1 signaling pathways in models of dysfunction caused by DOX- and ISO-induced cardiotoxicity, respectively [128, 129].

Myocardial infarction (MI) is a leading cause of mortality and is closely linked to oxidative damage and ferroptosis [130, 131]. Curdione effectively protects against ISO-induced MIBC (MI), evidenced by reduced MDA levels ($P < 0.05$, $P < 0.001$) and increased GPX4 expression ($P < 0.05$, $P < 0.01$, $P < 0.001$) at 25, 50, and 100 mg·kg^{-1}, as well as decreased iron content ($P < 0.01$) and increased GSH levels ($P < 0.01$) at 50 and 100 mg·kg^{-1}. Keap1 was identified as a direct target of curdione. Curdione disrupts the Keap1-Trx1 interaction while promoting Trx1-GPX4 complex formation, demonstrating that it inhibits ferroptosis in ISO-induced MI *via* the Keap1/Trx1/GPX4 pathway [132].

6.5. Neuroprotection

The neuroprotective effects of ZTO in cerebral ischemia are associated with enhanced anti-oxidant capacity, reduced delayed

neuronal death, inhibition of intravascular thrombosis, and attenuation of endothelial cell-mediated inflammation [133-135]. ZTO alleviates depression-like behavior by reducing oxidative stress and improving mitochondrial function *via* activation of the Nrf2/HO-1/NQO1 signaling pathway. Middle cerebral artery occlusion (MCAO) is a clinically relevant model of ischemic stroke, offering advantages such as minimal cranial trauma, controllable reperfusion, and high reproducibility. It is widely used in drug screening, novel therapy development, and mechanistic studies of cerebrovascular diseases like ischemia-reperfusion injury. Curdione (100 mg·kg^{-1}) significantly reduced infarct volume ($P < 0.01$, $P < 0.001$) on days 1, 4, 7, and 14 and improved neurological deficit scores ($P < 0.05$), cognitive recovery, and neuronal morphology in MCAO rats. Mechanistically, anti-oxidant and anti-apoptotic effects were involved, including increased SOD, CAT, and GSH-Px activities ($P < 0.05$) and decreased levels of cytochrome C (Cyt-C), Bax, c-caspase-9 ($P < 0.05$), and c-caspase-3 ($P < 0.01$) (Fig. 3) [136]. Despite its strengths, the MCAO model has limitations. Human stroke often involves multiple vessel occlusions, whereas MCAO typically targets only the middle cerebral artery. Reperfusion itself may cause additional injury. Therefore, complementary experimental models are necessary to fully evaluate curdione's neuroprotective potential.

6.6. Respiratory protection

The progression of pulmonary fibrosis is closely associated with the transforming growth factor-β (TGF-β1)/Smads signaling pathway [137, 138]. Overexpression of TGF-β induces myofibroblast differentiation, promotes ECM deposition, inhibits collagen degradation, and drives progressive fibrosis. Smads are cytoplasmic signal transduction proteins; Smad2 and Smad3 primarily mediate TGF-βR signaling activation and interact with numerous TGF-β-responsive promoters [139]. Curdione significantly reduced the Ashcroft score for fibrosis ($P < 0.01$) and down-regulated the expression of fibronectin ($P < 0.001$), collagen I ($P < 0.01$), and α-smooth muscle actin (α-SMA) ($P < 0.05$) in bleomycin-induced lung injury and fibrosis in C57BL/6 mice following intraperitoneal administration at 100 mg·kg^{-1}. *In vitro* assays demonstrated that curdione suppressed Smad3 phosphorylation ($P < 0.001$) and concentration-dependently reduced the expression of α-SMA, collagen I, and fibronectin ($P < 0.01$, $P < 0.001$). These findings indicate that curdione ameliorates bleomycin-induced pulmonary fibrosis by inhibiting TGF-β-driven fibroblast-to-myofibroblast differentiation [140].

Neutrophils are circulating effector cells in peripheral blood and play a critical role in immune defense against invading pathogens through phagocytosis, degranulation, and release of neutrophil extracellular traps (NETs). However, excessive NET formation can contribute to organ dysfunction and exacerbate sepsis-induced acute lung injury (SI-ALI) [141–143]. Studies have shown that curdione significantly alleviated histopathological changes ($P < 0.01$), attenuated inflammatory cytokine elevation ($P < 0.01$, $P < 0.001$, $P < 0.0001$), and reduced oxidative stress responses ($P < 0.01$, $P < 0.001$, $P < 0.0001$) in sepsis-induced lung injury after intraperitoneal administration at 50 or 100 mg·kg^{-1}. Furthermore, curdione inhibited platelet-mediated neutrophil recruitment, infiltration, and NET formation, suggesting its potential as a therapeutic agent for SI-ALI [144].

Ca^{2+}-activated chloride channels (CaCCs) regulate epithelial secretion, sensory signal transduction, neuronal excitability, and smooth muscle contraction, contributing to diverse physiological functions [145, 146]. Transmembrane protein 16A (TMEM16A) constitutes the molecular basis of a CaCC subgroup [147, 148]. It is highly expressed in inflammatory airway diseases and modulates mucin secretion and airway smooth muscle contraction [149–151]. Curdione inhibits TMEM16A channel activity in a dose-dependent manner, with an IC_{50} value of 14.45 μmol·L^{-1}. Intracellular Ca^{2+} elevation is essential for CaCC activation, and UTP induces Ca^{2+} release in airway epithelial cells. At 200 μmol·L^{-1}, curdione reduced UTP-stimulated Cl^- current from ~47 to ~17 μA·cm^{-2}. Inhibition of respiratory mucus hypersecretion may represent a novel mechanism by which curdione reduces airway obstruction and improves airway compliance *via* modulation of TMEM16A/ CaCC and CFTR channel activities [152].

6.7. Hepatoprotection

Curdione administered at 12.5, 25, and 50 mg·kg^{-1} prior to D-galactosamine (D-GalN)/LPS injection suppressed serum aspartate aminotransferase (AST) elevation ($P < 0.01$) and alanine aminotransferase (ALT) levels ($P < 0.05$, $P < 0.01$), while also mitigating D-GalN/LPS-induced liver necrosis in histological analyses. The hepatoprotective effect of curdione may be attributed to its protection of hepatocytes against D-GalN-induced toxicity [153, 154].

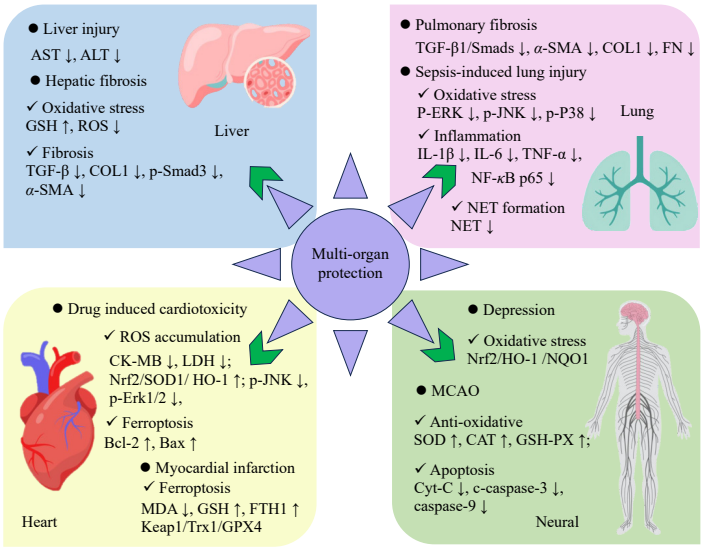

Fig. 3 Multi-organ protective effects of curdione. (↑) up-regulated; (↓) down-regulated. Relieving oxidative stress is common in multi-organ protective effects of curdione. TGF-β/Smads signaling pathway is down-regulated in the liver and pulmonary fibrosis. Ferroptosis and apoptosis are involved in the heart- and neuro-protective effects of curdione, respectively.

Activation of hepatic stellate cells (HSCs) into myofibroblasts leads to excessive ECM production and contributes to liver fibrosis. Autophagy, oxidative stress, and metabolic disturbances are implicated in HSC activation [155–158]. HSC-T6 cells, derived from rat HSCs, exhibit activated phenotypes characteristic of liver fibrosis progression. These cells display fibrotic features *in vitro*, including elevated *α*-actin and collagen synthesis, making them widely used in studies of liver fibrosis mechanisms and anti-fibrotic drug screening. Curdione significantly inhibited TNF-α-induced HSC activation and reduced the expression of *α*-SMA ($P < 0.001$), prostaglandin-endoperoxide synthase 2 (PTGS2) ($P < 0.001$), and p-Akt1 in HSC-T6 cells at concentrations of 150 and 300 μmol·L^{-1} [159]. Despite their widespread use, limitations such as species differences and phenotypic drift constrain the direct translation of HSC-T6 findings to human disease. Therefore, further studies are required to systematically evaluate the anti-fibrotic activity of curdione. Dai et al. reported that curdione (50 mg·kg^{-1}) enhanced the inhibitory effect of schisandrin C (Sin C) on hepatic fibrosis by modulating the TGF-β pathway and suppressing oxidative stress following 6 weeks of treatment, highlighting its potential in multi-target or multi-pathway combination therapies for liver fibrosis [160].

6.8. Anti-viral activity

Curdione demonstrates potent anti-influenza A (H1N1) activity in both *in vitro* and *in vivo* models. In A549 cells, curdione significantly reduced H1N1 viral mRNA and nucleoprotein expression in a dose-dependent manner across a concentration range of 1.56–100 μmol·L^{-1}. In an *in vivo* mouse model, intraperitoneal administration of curdione at 100 mg·kg^{-1} effectively attenuated H1N1-induced lung injury and suppressed viral replication by day 7 post-infection [161].

6.9. Anti-fungal activity

Phytophthora capsici (*P. capsici*) is a destructive oomycete pathogen causing severe disease in vegetables and various crops [162]. ZTO inhibits *P. capsici* growth and development *in vitro* by disrupting the cell membrane and inducing leakage of intracellular contents. ZTO also increased relative conductivity, MDA, and glycerol levels at concentrations of 2.5–20 μg·mL^{-1} after 24 h of incubation with mycelia. Further investigation revealed that curdione exerted moderate inhibitory effects on *P. capsici* mycelial growth in a concentration-dependent manner, achieving 49.23% inhibition at 20 μg·mL^{-1} [9].

Fusarium graminearum (*F. graminearum*) causes *Fusarium* head blight in wheat and barley and contaminates grains with mycotoxins, posing a public health risk [163, 164]. Although curdione constitutes only 0.87% of the extract from *Curcuma longa*, it demonstrated the strongest inhibitory effect on *F. graminearum* growth, with an inhibition rate of 52.9%. Disruption of fungal cell membrane integrity—specifically through inhibition of ergosterol synthesis and interference with the respiratory chain—underlies the anti-fungal mechanism of curdione against *F. graminearum* [165].

6.10. Anti-diabetic effect

Type 2 diabetes is a chronic condition characterized by insufficient insulin secretion or impaired insulin utilization. As the disease progresses, blood glucose levels rise progressively. Inhibiting *α*-glucosidase activity effectively controls postprandial glucose levels, making this enzyme a key therapeutic target for type 2 diabetes [166–169]. Curdione was evaluated for anti-diabetic activity using a glucose consumption assay in HepG2 cells. Results showed that curdione enhanced glucose consumption by over 60% at 10.0 μmol·L^{-1} [170]. Additionally, curdione content in extracts of *C. caesia* correlated strongly with *α*-glucosidase inhibitory activity [171]. These results suggest that curdione may serve as a promising alternative *α*-glucosidase inhibitor for reducing blood glucose levels and managing diabetes.

6.11. Hypertrophic scar alleviation

Hypertrophic scar fibroblasts (HSFs) typically arise after burns, scalds, or surgical procedures due to abnormal fibroblast proliferation, elevated pro-fibrotic factor expression, and dysregulated ECM secretion. This condition represents a common and challenging clinical skin disorder. The PI3K/Akt/mammalian target of rapamycin (mTOR) signaling pathway plays a central role in regulating cell proliferation and differentiation [172, 173]. Fibroblast proliferation promotes hypertrophic scar formation by stimulating collagen synthesis and fibrosis. The TGF-β1/Smad signaling pathway also critically regulates fibroblast proliferation, matrix secretion, and accumulation [174, 175]. Curdione inhibited HSF proliferation in a dose-dependent manner at 10, 20, and 40 μmol·L^{-1}, with a 70% inhibition rate observed at 40 μmol·L^{-1}. Moreover, it reduced COL-I and COL-III secretion ($P < 0.05$, $P < 0.01$) and decreased collagen accumulation by enhancing MMP-1 synthesis ($P < 0.05$, $P < 0.01$) in HSF cells at 20 and 40 μmol·L^{-1}, respectively. The expression levels of p-PI3K, p-Akt, p-mTOR, p-Smad3, TGF-β1, and *α*-SMA were also significantly suppressed by curdione in a dose-dependent manner ($P < 0.05$, $P < 0.01$). These results demonstrate that curdione alleviates hypertrophic scarring by inhibiting both the PI3K/Akt/mTOR and TGF-β1/Smads signaling pathways, indicating its potential for treating HSF [176].

7. Potential toxicities

7.1. Reproductive toxicity

SD rats received daily doses of 7, 21, or 63 mg·kg^{-1} curdione from gestational day 6 (GD_6) to GD_{15} to assess the toxicokinetic profile of curdione in pregnant rats and its transfer across the placental barrier. Results showed that c_{max}, $AUC_{(0-t)}$, and $AUC_{(0-\infty)}$ increased dose-dependently on both GD_6 and GD_{15}. Curdione was detected in maternal plasma, placental plasma, placental tissue, amniotic fluid, and fetal tissue. At 21 mg·kg^{-1}, curdione reached saturation in fetal tissue (236.10 ng·g^{-1}), suggesting a risk of accumulation in fetuses and potential transplacental transfer [177]. Wu et al. investigated the mechanism of curdione-induced reproductive toxicity in HTR-8/SVneo cells using multi-omics profiling. Exposure to curdione (500 or 1000 μmol·L^{-1}) induced mitochondrial dysfunction, DNA damage, and disruption of tight junctions, accompanied by down-regulation of Wnt6, *β*-catenin, claudin-1, and ZO-1. Modulation of the Wnt/*β*-catenin signaling pathway was implicated in curdione-induced cellular toxicity in HTR-8/SVneo cells [178].

7.2. Dyspnea

Dyspnea following drug administration is a typical adverse drug reaction (ADR) that has garnered global attention [179–181]. The primary adverse effects of ZTO injection (ZTOI) involve disorders of the respiratory system (45.63%), followed by systemic reactions and skin and appendage disorders. Among respiratory events, dyspnea accounts for 57.39% [182]. Yang et al. explored the mechanisms underlying ZTO-induced dyspnea and found that curdione binds to hemoglobin (Hb) with high affinity, exhibiting a predicted binding free energy of −6.9 kcal·mol^{-1}. Molecular docking indicated that curdione forms two conventional hydrogen bonds and is stabilized by four alkyl or π-alkyl hydrophobic inter-

actions with Trp37, Pro95, Lys127, and Ala130. Real-time interaction between curdione and Hb was confirmed by surface plasmon resonance (SPR), showing 1∶1 binding kinetics with an equilibrium dissociation constant (K_d) of 3.795 × 10^{-6} mol·L^{-1}, implicating Hb-based interference in ZTO-induced dyspnea [183]. While these interactions were validated *in vitro*, whether curdione-Hb binding alters Hb structure and function to induce dyspnea requires further *in vivo* investigation.

7.3. DDIs

DDIs commonly occur during combination therapy, potentially altering drug exposure or pharmacological effects [184]. DDIs may lead to therapeutic failure or adverse reactions [185, 186]. Cytochrome P450 (CYP450) enzymes metabolize various endogenous compounds and xenobiotics. Inhibition or induction of CYP450 isoforms is a major cause of clinically significant DDIs [187–189]. Studies show that curdione dose-dependently inhibits CYP3A4 activity within the range of 1–10 μg·mL^{-1}, with an IC_{50} of 10 μg·mL^{-1} in *in vitro* assays. Molecular analysis indicates that curdione interacts with CYP3A4 *via* hydrophobic contacts involving Arg105, Ser119, Hem1500, Ala370, Phe213, Arg212, and Phe304, and forms a hydrogen bond (3.06 Å) with imidazole. Additionally, curdione suppressed CYP3A4 protein expression in Caco-2 cells [190, 191]. Curdione reversibly inhibited CYP2B6 activity in a competitive manner, with an IC_{50} of 4.13 μmol·L^{-1}. Molecular docking revealed strong binding of curdione to the active site of human CYP2B6, with a binding energy of −8.34 kcal·mol^{-1}. The compound was surrounded by multiple hydrophobic residues, suggesting that hydrophobic interactions drive its binding to CYP2B6 [192].

8. Discussion and future persepectives

Curcuma is an important genus in the family Zingiberaceae. Several *Curcuma* species possess significant edible, medicinal, and economic value. Curdione is one of the primary bioactive constituents found in *Curcuma*. Its concentration varies across *Curcuma* species, geographical regions, plant parts, and extraction methods. The highest reported curdione content is 47.40% in the essential oil of *C. trichosantha*, indicating that curdione can be efficiently extracted and purified from natural sources. This offers advantages over chemical synthesis by reducing production costs and minimizing environmental pollution.

Curdione exhibits diverse therapeutic properties, including anti-thrombotic, anti-inflammatory, anticancer, anti-viral, antifungal, organ-protective, and anti-diabetic effects. It exerts antithrombotic activity by inhibiting platelet activation and aggregation through modulation of P-selectin levels and the AMPK-vinculin/talin-integrin αIIbβ3 signaling pathway. In PAF- and CAR-induced tail thrombosis mouse models, curdione (50 mg·kg^{-1}) demonstrated a thrombolytic effect comparable to clinical aspirin (100 mg·kg^{-1}), suggesting its potential as a therapeutic agent for thrombotic disorders. Inflammation plays a critical role in the progression of various chronic diseases. Curdione shows promise as a complementary treatment for inflammation-related conditions, primarily through mechanisms involving attenuation of oxidative stress, suppression of macrophage M1 polarization, and inhibition of the NF-κB signaling pathway. Additionally, curdione displays cytotoxicity against multiple cancer cell lines by inhibiting proliferation and inducing autophagy and ferroptosis, mediated *via* regulation of MAPKs and PI3K/Akt signaling pathways, as well as key molecules such as p53, IDO1, MMP-2/9 axis, CA2, SLC7A11, and METTL14. These findings highlight its potential as a candidate for anticancer therapy. However, current studies, although promising, lack sufficient depth to fully elucidate the underlying mechanisms of its anticancer activity. Moreover, most experiments lack positive controls, which may compromise the accuracy and comprehensiveness of curdione's efficacy evaluation due to the absence of valid reference benchmarks.

Despite its broad pharmacological profile, several challenges hinder the commercialization and clinical application of curdione. As a sesquiterpenoid with a germacrene skeleton, curdione contains double bonds that render it susceptible to tautomerism. These structural features contribute to poor water solubility and low stability—key limitations for clinical development. Selective introduction of hydrophilic groups represents a viable strategy to enhance curdione's aqueous solubility. Chemo-bio transformation enables regio- and stereo-selective modification of natural products, offering opportunities for precise structural optimization of curdione. Nevertheless, further investigation into the biological activities of modified derivatives and structure–activity relationship (SAR) studies are required to improve both stability and pharmacological potency. Emerging technologies, such as cocrystallization to form binary crystal structures with specific ligands or encapsulation within cyclodextrin cavities to create inclusion complexes, also hold promise for enhancing the solubility and stability of curdione.

Pharmacokinetic parameters of curdione have primarily been derived following administration of ZTO or *Curcuma* extracts, potentially overlooking component interactions. Furthermore, most existing data represent preliminary findings and do not adequately reflect the complete absorption, distribution, metabolism, and excretion (ADME) profile of curdione *in vivo*. Therefore, systematic and comprehensive pharmacokinetic studies are warranted. Following intravenous administration, curdione exhibits rapid absorption and elimination characteristics *in vivo*. While fast absorption may enable prompt therapeutic effects, it could also lead to adverse reactions due to a sharp rise in blood concentration over a short period. Additionally, rapid absorption may accelerate drug metabolism and shorten half-life. Given its quick elimination, maintaining stable plasma concentrations might require increased dosing frequency or higher doses. Application of sustained-release delivery systems—such as liposomes, microspheres, microemulsions, and nanoemulsions—offers multiple benefits, including improved patient compliance, reduced dosing frequency, and enhanced drug targeting, thereby potentially optimizing the *in vivo* pharmacokinetics of curdione.

Curdione accumulates in placental plasma in a dose-dependent manner and crosses the placental barrier into fetal tissues, raising concerns about its use during pregnancy. *In vitro* assays indicate that curdione induces reproductive toxicity in HTR-8/SVneo cells by modulating oxidative stress, causing mitochondrial dysfunction, and disrupting tight junctions *via* the Wnt/β-catenin signaling pathway. These findings suggest potential reproductive risks; however, certain limitations remain. Accumulation in fetal tissue alone does not constitute direct evidence of reproductive toxicity, as primary indicators—such as congenital abnormalities, developmental delays, or postnatal growth impairments—are lacking. Thus, additional data on fetal development, growth trajectories, and histopathological changes are necessary. Moreover, the curdione concentrations used in pharmacokinetic and *in vitro* mechanistic studies often exceed clinically relevant dosages. Consequently, whether curdione elicits reproductive toxicity at therapeutic levels requires further systematic *in vivo* evaluation. Molecular docking and SPR analyses reveal that curdione has high affinity for Hb (K_d, 3.795 × 10^{-6} mol·L^{-1}), suggesting a potential risk of dyspnea. However, these *in vitro* systems involve only curdione and Hb, whereas real blood contains numerous competing components. Interactions with other blood constituents, such as platelets, may reduce curdione's binding to Hb. Furthermore, its rapid absorption, distribution, metabolism, and elimination likely limit prolonged exposure to Hb. Considering these factors, current evidence is insufficient to conclude that

curdione induces dyspnea. Further *in vivo* investigations are needed to systematically assess this possibility. DDI assessment is a critical step in new drug development, providing a scientific basis for clinical trial design and eventual commercialization. *In vitro* studies show that curdione inhibits CYP2B6 and CYP3A4, indicating a potential for DDIs when co-administered with drugs metabolized by these enzymes. However, *in vitro* models cannot fully replicate the complex physiological and pathological environments present in animals or humans. Additionally, current DDI research on curdione focuses predominantly on CYP450 enzymes, neglecting broader metabolic pathways and transporter systems. Therefore, a comprehensive toxicity evaluation—particularly under chronic administration, across dose-response relationships, and at the mechanistic level—is essential before advancing to clinical trials.

In summary, curdione is widely distributed among *Curcuma* species and readily obtainable from natural sources. It demonstrates multiple promising pharmacological activities, including anticancer, anti-thrombotic, and anti-inflammatory effects. Nevertheless, significant challenges must be addressed before progressing to clinical trials. Future research should prioritize improving solubility and stability, clarifying the mechanisms underlying its pharmacological actions, and conducting systematic toxicological evaluations.

Funding

This work was supported by the National Natural Science Foundation of China (Nos. 82192913 and 82304851), the Scientific and Technological Innovation Project of China Academy of Chinese Medical Sciences (Nos. CI2023E002, CI2021B016, and CI2021A04801), and the Fundamental Research Funds for the Central Public Welfare Research Institutes (Nos. ZZ13-YQ-055 and ZXKT22044).

Declaration of competing interest

These authors have no conflict of interest to declare.

References

1 Chopra B, Dhingra AK. Natural products: a lead for drug discovery and development. *Phytother Res*. 2021;35(9):4660-4702. https://doi.org/10.1002/ptr.7099.
2 Wang XL. Clinical effect observation of microwave and confort pessaries combination to chronic cervicitis. *Chin Contin Med Edu*. 2015;7(7):235-236. https://doi.org/10.3969/j.issn.1674-9308.2015.07.199.
3 Wang ZQ. Curative effect observation on treatment of 180 cases of vaginitis patients Compound Zedoary Turmeric Oil Suppoaitories. *World Latest Med Inf*. 2015;15(11):7-8. https://doi.org/10.3969/j.issn.1671-3141.2015.11.005.
4 Yuan FL, Xu YY, Jiang CX. Meta analysis of comparison between zedoary turmeric oil injection and ribavirin injection in treatment of viral lower respiratory tract infections in children. *Chin Tradit Herbal Drugs*. 2024;55(12):4132-4139. https://doi.org/10.7501/j.issn.0253-2670.2024.12.020.
5 Wang L, Tang SW, Xu H, et al. Efficacy and safety of zedoray turmeric oil injection in the treatment of rotavirus enteritis: a meta-analysis. *Chin Pharm*. 2019;28(7):65-68. https://doi.org/10.3969/j.issn.1006-4931.2019.07.021.
6 Zhang XJ, Xu FX, Ding MX, et al. Clinical observation of zedoary turmeric oil injection in treating cases of influenza. *J Gannan Med Univ*. 2019;39(12):1220-1222. https://doi.org/10.3969/j.issn.1001-5779. 2019.12.008.
7 Zhao WQ. Effect of CAP chemotherapy combined with zedoary oil injection on quality of life in patients with early high-risk endometrial carcinoma. *Jilin Med J*. 2019;40(9):2020-2021.
8 Liang D, Yang MC, Lin Z, et al. Effect observation on treating ovarian cancer with curcuma oil injection plus conventional chemotherapy. *Clin J Chin Med*. 2014;6(4):7-8. https://doi.org/10.3969/j.issn.1674-7860.2014.04.003.
9 Wang B, Liu F, Li Q, et al. Antifungal activity of zedoary turmeric oil against *Phytophthora capsici* through damaging cell membrane. *Pestic Biochem Physiol*. 2019;159:59-67. https://doi.org/10.1016/j.pestbp.2019.05.014.
10 Hu YC, Zhang JM, Kong WJ, et al. Mechanisms of antifungal and anti-aflatoxigenic properties of essential oil derived from turmeric (*Curcuma longa* L.) on *Aspergillus flavus*. *Food Chem*. 2017;220:1-8. https://doi.org/10.1016/j.foodchem.2016.09.179.
11 Zhang SH, Liu D, Zhou YK, et al. Analysis of *Curcuma wenyujin* oil components with different extration method by GC-Q/TOF-MS. *Cent South Pharm*. 2020;18(11):1879-1887. https://doi.org/10.7539/j.issn.1672-2981.2020.11.021.
12 Wang F, Sun Z, Zhang QY, et al. Curdione induces ferroptosis mediated by m6A methylation *via* METTL14 and YTHDF2 in colorectal cancer. *Chin Med*. 2023;18(1):122. https://doi.org/10.1186/s13020-023-00820-x.
13 Wei W, Rasul A, Sadiqa A, et al. Curcumol: from plant roots to cancer roots. *Int J Biol Sci*. 2019;15(8):1600-1609. https://doi.org/10.7150/ijbs.34716.
14 Li J, Sun YT, Li GH, et al. The extraction, determination, and bioactivity of curcumenol: a comprehensive review. *Molecules*. 2024;29(3):656. https://doi.org/10.3390/molecules29030656.
15 Luo YH, Wang ZC, Jiang JE, et al. Curzerene suppresses hepatocellular carcinoma progression through the PI3K/AKT/MTOR pathway. *Rev Invest Clin*. 2024;76(4):173-184. https://doi.org/10.24875/RIC.24000018.
16 Lou GH, Huang Y, Wang Y, et al. Germacrone, a novel and safe anticancer agent from genus *Curcuma*: a review of its mechanism. *Anticancer Agents Med Chem*. 2023;23(13):1490-1498. https://doi.org/10.2174/1871520623666230420094628.
17 Feng YW, An QW, Zhao ZQ, et al. *β*-Elemene: a phytochemical with promise as a drug candidate for tumor therapy and adjuvant tumor therapy. *Biomed Pharmacother*. 2024;172:116266. https://doi.org/10.1016/j.biopha.2024.116266.
18 Lv XY, Sun JC, Hu LF, et al. Curcumol inhibits malignant biological behaviors and TMZ-resistance in glioma cells by inhibiting long noncoding RNA FOXD2-As1-promoted EZH2 activation. *Aging*. 2021;13(21):24101-24116. https://doi.org/10.18632/aging.203662.
19 Pan J, Miao D, Chen L. Germacrone reverses adriamycin resistance in human chronic myelogenous leukemia K562/ADM cells by suppressing MDR1 gene/P-glycoprotein expression. *Chem Biol Interact*. 2018;288:32-37. https://doi.org/10.1016/j.cbi.2018.04.012.
20 Zhang RN, Zheng YT, Zhu QR, et al. *β*-Elemene reverses gefitinib resistance in NSCLC cells by inhibiting lncRNA H19-mediated autophagy. *Pharmaceuticals*. 2024;17(5):626. https://doi.org/10.3390/ph17050626.
21 Zhang QZ, Yang F, Zhu JJ, et al. Essential oil composition of three herbal medicines from *Curcumal wenyujin* by GC-MS. *Chin J Chin Mater Med*. 2010;35(19):2590-2593.
22 Zang YF, Xu LL, Liu HC, et al. Determination of 8 main active compounds in Curcumae Rhizoma by HPLC wavelength switching method. *Chin J Mod Appl Pharm*. 2021;38(18):2227-2233. https://doi.org/10.13748/j.cnki.issn1007-7693.2021.18.006.
23 Ravindran PN, Babu KN, Sivaraman K. Turmeric: the genus *Curcuma*. 1st Ed. Boca Raton, BR: CRC Press; 2007. https://doi.org/10.1201/9781420006322.
24 Anggriani L, Yasmin A, Wulandari AR, et al. Extract of temu ireng (*Curcuma aeruginosa* Roxb.) rhizome reduces doxorubicin-induced immunosuppressive effects. *AIP Conf Proc*. 2019;2099(1):020001. https://doi.org/10.1063/1.5098406.
25 Tabtipwon P, Temsiririrkkul R, Thongpraditchote S, et al. Anti-inflammatory activity of *Curcuma cf. amada* roxb. 'Wan en Lueang'. *Pharm Sci Asia*. 2020;47(2):121-129. https://doi.org/10.29090/psa.2020.02.018.0051.
26 Kojima H, Yanai T, Toyota A. Essential oil constituents from Japanese and Indian *Curcuma aromatica* rhizomes. *Planta Med*. 1998;64(4):380-381. https://doi.org/10.1055/s-2006-957458.
27 Albaqami JJ, Hamdi H, Narayanankutty A, et al. Chemical composition and biological activities of the leaf essential oils of *Curcuma longa, Curcuma aromatica* and *Curcuma angustifolia*. *Antibiotics*. 2022;11(11):1547. https://doi.org/10.3390/antibiotics11111547.
28 Dung N, Truong P, Ky PT, et al. Chemical composition of the essential oils of *Curcuma cochinchinensis* Gagnep. from Vietnam. *ACGC Chem Res Commun*. 1996;5:11-16.
29 Dũng NX, Truong PX, Ky PT, et al. Volatile constituents of the leaf, stem, rhizome, roof and flower oils of *Curcuma harmandii* gagnep. from Vietnam. *J Essent Oil Res*. 1997;9(6):677-681. https://doi.org/10.1080/10412905.1997.9700810.
30 Zhang LY, Yang ZW, Wei JW, et al. Contrastive analysis of chemical composition of essential oil from twelve Curcuma species distributed in China. *Ind Crops Prod*. 2017;108:17-25. https://doi.org/10.1016/j.indcrop.2017.06.005.
31 Devi LR, Rana VS, Devi SI, et al. Chemical composition and antimicrobial activity of the essential oil of *Curcuma leucorhiza* Roxb. *J Essent Oil Res*. 2012;24(6):533-538. https://doi.org/10.1080/10412905.2012.728089.
32 Thánh KP, van de Ven, LJM, Leclercq PA, et al. Volatile constituents of the essential oil of *Curcuma trichosantha* gagnep. from Vietnam. *J Essent Oil Res*. 1994;6(2):213-214. https://doi.org/10.1080/10412905.1994.9698361.
33 Thu NT, Tran-Trung H, Duc DX, et al. Rhizome essential oil of *Curcuma zedoaroides* Chaveer. & Tanee: chemical composition, cytotoxic activities, and molecular docking approach. *J Essent Oil Res*. 2024;27(1):188-197. https://doi.org/10.1080/0972060X.2024.2314554.
34 Zhou L, Zhang KW, Li J, et al. Inhibition of vascular endothelial growth factor-mediated angiogenesis involved in reproductive toxicity induced by sesquiterpenoids of *Curcuma zedoaria* in rats. *Reprod Toxicol*. 2013;37:62-69. https://doi.org/10.1016/j.reprotox.2013.02.001.
35 Nuzula AF, Kristanti AN, Aminah NS, et al. Isolation and strucure elucidation of secondary metabolite compounds from *Curcuma aeruginosa*. *J Kimia Riset*. 2023;8:81-91. https://doi.org/10.20473/jkr.v8i1.44073.
36 Giang PM, Son PT, Matsunami K, et al. New sesquiterpenoids from *Curcuma aff. aeruginosa* Roxb. *Heterocycles*. 2007;74:977-981. https://doi.org/10.3987/COM-07-S(W)42.
37 Jirovetz L, Buchbauer G, Puschmann C, et al. Essential oil analysis of *Curcuma aeruginosa* roxb. leaves from South India. *J Essent Oil Res*. 2000;12(1):47-49. https://doi.org/10.1080/10412905.2000.9712039.
38 Herath H, Wijayasiriwardene T, Premakumara G. GC-MS identification of endemic herb *Curcuma albiflora* THW. (Sri Lanka). *Int J Pharmacogn*. 2018;5(7):419-425. https://doi.org/10.13040/ijpsr.0975-8232.ijp.5(7).419-425.
39 Herath H, Wijayasiriwardene T, Premakumara G. Comparative GC-MS analysis of all *Curcuma* species grown in Sri Lanka by multivariate test.

Ruhuna J Sci. 2017;8(2):103. https://doi.org/10.4038/rjs.v8i2.29.
40 Srivastava AK, Srivastava SK, Syamsundar KV. Volatile composition of *Curcuma angustifolia* roxb. rhizome from central and southern India. *Flavour Frag J*. 2006;21(3):423-426. https://doi.org/10.1002/ffj.1680.
41 Qu Y, Xu FM, Nakamura S, et al. Sesquiterpenes from *Curcuma comosa*. *J Nat Med*. 2009;63(1):102-104. https://doi.org/10.1007/s11418-008-0282-8.
42 Ratchanaporn C, Prapapan P, Pawinee P, et al. Cytotoxic sesquiterpenoids and diarylheptanoids from the rhizomes of *Curcuma elata* Roxb. *Rec Nat Prod*. 2014;8(1):46-50.
43 Raj G, Baby S, Dan M, et al. Volatile constituents from the rhizomes of *Curcuma haritha* Mangaly and Sabu from southern India. *Flavour Frag J*. 2008;23(5):348-352. https://doi.org/10.1002/ffj.1891.
44 Malek SN, Seng CK, Zakaria Z, et al. The essential oil of *Curcuma inodora* aff. Blatter from Malaysia. *J Essent Oil Res*. 2006;18(3):281-283. https://doi.org/10.1080/10412905.2006.9699088.
45 Keeratinijakal V, Kongkiatpaiboon S. Distribution of phytoestrogenic diarylheptanoids and sesquiterpenoids components in *Curcuma comosa* rhizomes and its related species. *Rev Bras Farmacogn*. 2017;27(3):290-296. https://doi.org/10.1016/j.bjp.2016.12.003.
46 Mohammad NHS, Aspollah SM, Safinar II, et al. *In vitro* cytotoxic, radical scavenging and antimicrobial activities of *Curcuma mangga* valeton and van zijp. *Int J Med Toxico Legal Med*. 2020;23:251-256. https://doi.org/10.5958/0974-4614.2020.00036.4.
47 Nguyen MC, Vu TH, Pham NK, et al. Chemical compositions and antimicrobial activity of essential oil from the rhizomes of *Curcuma singularis* growing in Vietnam. *Am J Essent Oil Nat Prod*. 2017;5(4):20-25.
48 Hikino H, Sakurai Y, Takahashi H, et al. Structure of curdione. *Chem Pharm Bull*. 1966;14(11):1310-1311. https://doi.org/10.1248/cpb.14.1310.
49 Zhao RB, Wu YL. Total synthesis of (−)-Curdione. *Acta Chim Sin*. 1988;46:615-616.
50 Zhou QM, Wang WH, Xia P, et al. Content determination of six chemical components in Curcuma Rhizoma under different storage conditions by HPLC. *China Pharm*. 2020;23(8):1669-1673.
51 Ji ZZ, Zeng ZJ. A quantitative conversion from curdione into curcumol. *J Shenyang Pharm Univ*. 1985;2(1):56-60. https://doi.org/10.14066/j.cnki.cn21-1349/r.1985.01.011.
52 Zhou Y, Chen P, Lei M, et al. The optimization on transformation from curdione to curcumol. *J Wuhan Polytech Univ*. 2017;36(1):30-33. https://doi.org/10.3969/j.issn.2095-7386.2017.01.006.
53 David CB, Luis C, lan C, et al. Organic synthesis provides opportunities to transform drug discovery. *Nat Chem*. 2018;10(4):383-394. https://doi.org/10.1038/s41557-018-0021-z.
54 Chen YN, Zhang L, Qin B, et al. An insight into the curdione biotransformation pathway by *Aspergillus niger*. *Nat Prod Res*. 2014;28(7):454-460. https://doi.org/10.1080/14786419.2013.873434.
55 Ma XC, Zheng J, Wu LJ, et al. Structural determination of three new germacrane-type sesquiterpene alcohols from curdione by microbial transformation. *Magn Reson Chem*. 2007;45(1):90-92. https://doi.org/10.1002/mrc.1922.
56 Qin B, Li YX, Meng LX, et al. "Mirror-image" manipulation of curdione stereoisomer scaffolds by chemical and biological approaches: development of a sesquiterpenoid library. *J Nat Prod*. 2015;78(2):272-278. https://doi.org/10.1021/np500864e.
57 Guo F, Xu F, Yu JH, et al. Metabolism and distribution of two major constituents of 'Xing-Nao-Jing Injection'-germacrone and curdione in rats. *J Pharm Biomed Anal*. 2024;248:116288. https://doi.org/10.1016/j.jpba.2024.116288.
58 You J, Li QP, Yu YW, et al. Absorption of zedoary oil in rat intestine using in situ single pass perfusion model. *Acta Pharm Sin*. 2004;39(10):849-853. https://doi.org/10.16438/j.0513-4870.2004.10.018.
59 Li WJ, Hong B, Li ZJ, et al. GC-MS method for determination and pharmacokinetic study of seven volatile constituents in rat plasma after oral administration of the essential oil of Rhizoma Curcumae. *J Pharm Biomed Anal*. 2018;149:577-585. https://doi.org/10.1016/j.jpba.2017.11.058.
60 Li JC, Mao CQ, Li L, et al. Pharmacokinetics and liver distribution study of unbound curdione and curcumol in rats by microdialysis coupled with rapid resolution liquid chromatography (RRLC) and tandem mass spectrometry. *J Pharm Biomed Anal*. 2014;95:146-150. https://doi.org/10.1016/j.jpba.2014.02.025.
61 Peng Y, Zhang M, Li WW, et al. A validated LC-MS/MS assay for the quantitative determination of curdione in rabbit plasma and its application to a pharmacokinetic study after administration of zedoary turmeric oil and bioavailability of the oil. *Biomed chromatogr*. 2014;28(10):1360-1365. https://doi.org/10.1002/bmc.3175.
62 Zhang KY, LV LL, Chen JX, et al. Effect of curdione on MDA-MB-231 cell cycle and apoptosis. *Chin J Exp Tradit Med Form*. 2021;27(12):74-81. https://doi.org/10.13422/j.cnki.syfjx.20211298.
63 Engeland K. Cell cycle arrest through indirect transcriptional repression by p53: I have a DREAM. *Cell Death Differ*. 2018;25(1):114-132. https://doi.org/10.1038/cdd.2017.172.
64 Wei C, Li DH, Liu Y, et al. Curdione induces antiproliferation effect on human uterine leiomy osarcoma targeting IDO1. *Front Oncol*. 2021;11:637024. https://doi.org/10.3389/fonc.2021.637024.
65 Wang JL, Wang X, Xia Q, et al. Study on the inhibitory effect of three sesquiterpenoids in Zedoary turmeric oil on hepatocellular carcinoma HepG2 cells. *Chin Tradit Pat Med*. 2014;36(7):1535-1539. https://doi.org/10.3969/j.issn.1001-1528.2014.07.045.
66 Mahmoud G, Esen E, Hugh JB, et al. Raman spectroscopy detects biochemical changes due to different cell culture environments in live cells *in vitro*. *Anal Bioanal Chem*. 2018;410(28):7537-7550. https://doi.org/10.1007/s00216-018-1371-5.
67 Teresa LS, Paulo JO, Vilma AS, et al. Different concentrations of berberine result in distinct cellular localization patterns and cell cycle effects in a melanoma cell line. *Cancer Chemother Pharmacol*. 2008;61(6):1007-1018. https://doi.org/10.1007/s00280-007-0558-9.
68 Li J, Bian WH, Wan J, et al. Curdione inhibits proliferation of MCF-7 cells by inducing apoptosis. *Asian Pac J Cancer Prev*. 2014;15(22):9997-10001. https://doi.org/10.7314/APJCP.2014.15.22.9997.
69 Zhai LJ, Spranger S, Binder DC, et al. Molecular pathways: targeting IDO1 and other tryptophan dioxygenases for cancer immunotherapy. *Clin Cancer Res*. 2015;21(24):5427-5433. https://doi.org/10.1158/1078-0432.CCR-15-0420.
70 Sun CT, Li MZ, Zhang L, et al. IDO1 plays a tumor-promoting role *via* MDM2-mediated suppression of the p53 pathway in diffuse large B-cell lymphoma. *Cell Death Dis*. 2022;13(6):572. https://doi.org/10.1038/s41419-022-05021-2.
71 Wang HM, Luo YY, Ran R, et al. IDO1 modulates the sensitivity of epithelial ovarian cancer cells to cisplatin through ROS/p53-dependent apoptosis. *Int J Mol Sci*. 2022;23(19):12002. https://doi.org/10.3390/ijms231912002.
72 Yang YR, Jin Y, Yin LZ, et al. Sertaconazole nitrate targets IDO1 and regulates the MAPK signaling pathway to induce autophagy and apoptosis in CRC cells. *Eur J Pharmacol*. 2023;942:175515. https://doi.org/10.1016/j.ejphar.2023.175515.
73 Jiang NN, Dai QJ, Su XR, et al. Role of PI3K/AKT pathway in cancer: the framework of malignant behavior. *Mol Biol Rep*. 2020;47(6):4587-4629. https://doi.org/10.1007/s11033-020-05435-1.
74 He Y, Sun MM, Zhang GG, et al. Targeting PI3K/Akt signal transduction for cancer therapy. *Signal Transduct Target Ther*. 2021;6(1):425. https://doi.org/10.1038/s41392-021-00828-5.
75 Wang P, Zhao WB, Wang YD. Inhibition proliferation and induced apoptosis effects of curdione on carcinom renal ACHN cells through PI3K/Akt signaling pathway. *Chin J Tradit Med Sci Tech*. 2020;27(2):196-199.
76 Wang CC, Guo J, Wu ZA. Combinative treatment of curdione and docetaxel triggers reactive oxygen species (ROS)-mediated intrinsic apoptosis of triple-negative breast cancer cells. *Bioengineered*. 2021;12(2):10037-10048. https://doi.org/10.1080/21655979.2021.1994737.
77 Glick D, Barth S, Macleod KF. Autophagy: cellular and molecular mechanisms. *J Pathol*. 2010;221(1):3-12. https://doi.org/10.1002/path.2697.
78 Liu SZ, Yao SJ, Yang H, et al. Autophagy: regulator of cell death. *Cell Death Dis*. 2023;14(10):648. https://doi.org/10.1038/s41419-023-06154-8.
79 Onorati AV, Dyczynski M, Ojha R, et al. Targeting autophagy in cancer. *Cancer*. 2018;124(16):3307-3318. https://doi.org/10.1002/cncr.31335.
80 Bravo-Cordero JJ, Hodgson L, Condeelis J. Directed cell invasion and migration during metastasis. *Curr Opin Cell Biol*. 2012;24(2):277-283. https://doi.org/10.1016/j.ceb.2011.12.004.
81 Webb AH, Gao BT, Goldsmith ZK, et al. Inhibition of MMP-2 and MMP-9 decreases cellular migration, and angiogenesis in *in vitro* models of retinoblastoma. *BMC Cancer*. 2017;17(1):434. https://doi.org/10.1186/s12885-017-3418-y.
82 Li XY, Huang GH, Liu QK, et al. Porf-2 inhibits tumor cell migration through the MMP-2/9 signaling pathway in neuroblastoma and glioma. *Front Oncol*. 2020;10:975. https://doi.org/10.3389/fonc.2020.00975.
83 Eidizade F, Soukhtanloo M, Zhiani R, et al. Inhibition of glioblastoma proliferation, invasion, and migration by Urolithin B through inducing G_0/G_1 arrest and targeting MMP-2/-9 expression and activity. *Biofactors*. 2023;49(2):379-389. https://doi.org/10.1002/biof.1915.
84 Sun XR, Yang K, Lv LL, et al. Effect and mechanism of curdione on migration and invasion of breast cancer HCC1937 cells. *Chin J Exp Tradit Med Form*. 2019;25(3):66-73. https://doi.org/10.13422/j.cnki.syfjx.20190326.
85 Jiang E, Wang Z. Study of curdione on proliferation, apoptosis and invasion of human cervical carcinoma HeLa cells. *Jilin Med J*. 2021;42(5):1032-1034. https://doi.org/10.3969/j.issn.1004-0412.2021.05.002.
86 Tachibana H, Gi M, Kato M, et al. Carbonic anhydrase 2 is a novel invasion-associated factor in urinary bladder cancers. *Cancer Sci*. 2017;108(3):331-337. https://doi.org/10.1111/cas.13143.
87 Chi BJ, Duan ZL, Hasan A, et al. Effect and mechanism of curdione combined with gemcitabine on migration and invasion of bladder cancer. *Biochem Genet*. 2024;62(4):2933-2945. https://doi.org/10.1007/s10528-023-10584-6.
88 Jiang XJ, Stockwell BR, Conrad M. Ferroptosis: mechanisms, biology and role in disease. *Nat Rev Mol Cell Biol*. 2021;22(4):266-282. https://doi.org/10.1038/s41580-020-00324-8.
89 Mou YH, Wang J, Wu JC, et al. Ferroptosis, a new form of cell death: opportunities and challenges in cancer. *J Hematol Oncol*. 2019;12(1):34. https://doi.org/10.1186/s13045-019-0720-y.
90 Zhang C, Liu XY, Jin SD, et al. Ferroptosis in cancer therapy: a novel approach to reversing drug resistance. *Mol Cancer*. 2022;21(1):47. https://doi.org/10.1186/s12943-022-01530-y.
91 Liu Y, Wan YC, Jiang Y, et al. GPX4: the hub of lipid oxidation, ferroptosis, disease and treatment. *Biochim Biophys Acta Rev Cancer*. 2023;1878(3):188890. https://doi.org/10.1016/j.bbcan.2023.188890.
92 Zhang WZQ, Liu Y, Liao Y, et al. GPX4, ferroptosis, and diseases. *Biomed Pharmacother*. 2024;174:116512. https://doi.org/10.1016/j.biopha.2024.116512.
93 Fan ZY, Yang GW, Zhang W, et al. Hypoxia blocks ferroptosis of hepatocellular carcinoma *via* suppression of METTL14 triggered YTHDF2-dependent silencing of SLC7A11. *J Cell Mol Med*. 2021;25(21):10197-10212. https://doi.org/10.1111/jcmm.16957.
94 Melincovici CS, Boşca AB, Şuşman S, et al. Vascular endothelial growth factor (VEGF)-key factor in normal and pathological angiogenesis. *Rom J Morphol Embryol*. 2018;59(2):455-467.
95 Yao DF, Wu XH, Zhu Y, et al. Quantitative analysis of vascular endothelial growth factor, microvascular density and their clinicopathologic features in human hepatocellular carcinoma. *Hepatobiliary Pancreat Dis Int*. 2005;4(2):220-226.
96 Fernández M, Semela D, Bruix J, et al. Angiogenesis in liver disease. *J Hepatol*. 2009;50(3):604-620. https://doi.org/10.1016/j.jhep.2008.12.011.
97 Zou Y, Guo CG, Yang ZG, et al. A small interfering RNA targeting vascular

endothelial growth factor efficiently inhibits growth of VX2 cells and VX2 tumor model of hepatocellular carcinoma in rabbit by transarterial embolization-mediated siRNA delivery. *Drug Des Devel Ther*. 2016;10:1243-1255. https://doi.org/10.2147/dddt.s94122.
98 Cao RR, Zhou J, Wang QM, et al. The effect of the curdione on the proliferation of HHSEC under the microenvironment of HepG2 cells *via* VEGF/VEGFR2 signaling pathway. *J Hunan Univ Chin Med*. 2021;41(12): 1835-1839. https://doi.org/10.3969/j.issn.1674－070X.2021.12.004.
99 Merten M, Thiagarajan P. P-selectin expression on platelets determines size and stability of platelet aggregates. *Circulation*. 2000;102(16):1931-1936. https://doi.org/10.1161/01.CIR.102.16.1931.
100 Tan TF, Cheng ZW, Han GW, et al. Study on intracellular uptake of curdione in platelets. *J Pharm Anal*. 2023;43(2):253-261. https://doi.org/10.16155/j.0254-1793.2023.02.09.
101 Tong HJ, Yu MT, Fei CH, et al. Bioactive constituents and the molecular mechanism of Curcumae Rhizoma in the treatment of primary dysmenorrhea based on network pharmacology and molecular docking. *Phytomedicine*. 2021;86:153558. https://doi.org/10.1016/j.phymed.2021.153558.
102 Xia Q, Dong TX, Zhan HQ, et al. Inhibition effect of curdione on platelet aggregation induced by ADP in rabbits. *Chin Pharmacol Bull*. 2006;22(9): 1151-1152.
103 Wang X, Xia Q, Xu DJ, et al. Study on anticoagulant and antithrombotic effects of curdione in *Curcuma*. *Chin Tradit Pat Med*. 2012;34(3):550-553.
104 Xia Q, Wang X, Xu DJ, et al. Inhibition of platelet aggregation by curdione from *Curcuma wenyujin* essential Oil. *Thromb Res*. 2012;130(3):409-414. https://doi.org/10.1016/j.thromres.2012.04.005.
105 Bennett JS. Regulation of integrins in platelets. *Biopolymers*. 2015;104(4): 323-333. https://doi.org/10.1002/bip.22679.
106 Huang JS, Li X, Shi XF, et al. Platelet integrin αIIbβ3: signal transduction, regulation, and its therapeutic targeting. *J Hematol Oncol*. 2019;12(1):26. https://doi.org/10.1186/s13045-019-0709-6.
107 Janus-Bell E, Mangin PH. The relative importance of platelet integrins in hemostasis, thrombosis and beyond. *Haematologica*. 2023;108(7):1734-1747. https://doi.org/10.3324/haematol.2022.282136.
108 Nieswandt B, Moser M, Pleines I, et al. Loss of talin1 in platelets abrogates integrin activation, platelet aggregation, and thrombus formation *in vitro* and *in vivo*. *J Exp Med*. 2007;204(13):3113-3118. https://doi.org/10.1084/jem.20071827.
109 Petrich BG, Marchese P, Ruggeri ZM, et al. Talin is required for integrin-mediated platelet function in hemostasis and thrombosis. *J Exp Med*. 2007;204(13):3103-3111. https://doi.org/10.1084/jem.20071800.
110 Nanda SY, Hoang T, Patel P, et al. Vinculin regulates assembly of talin: β3 integrin complexes. *J Cell Biochem*. 2014;115(6):1206-1216. https://doi.org/10.1002/jcb.24772.
111 Kimmerlin Q, Moog S, Yakusheva A, et al. Loss of α4A- and β1-tubulins leads to severe platelet spherocytosis and strongly impairs hemostasis in mice. *Blood*. 2022;140(21):2290-2299. https://doi.org/10.1182/blood.2022016729.
112 Cuenca-Zamora EJ, Ferrer-Marín F, Rivera J, et al. Tubulin in platelets: when the shape matters. *Int J Mol Sci*. 2019;20(14):3484. https://doi.org/10.3390/ijms20143484.
113 Zhang DL, Qiao WH, Zhao YL, et al. Curdione attenuates thrombin-induced human platelet activation: β1-tubulin as a potential therapeutic target. *Fitoterapia*. 2017;116:106-115. https://doi.org/10.1016/j.fitote.2016.11.016.
114 Cheng ZW, Shi HB, Liu QH, et al. Inhibitory effect of curdione on thrombine-induced activation of human platelet integrin α Ⅱ bβ3. *Chin Tradit Pat Med*. 2024;46(6):2038-2041. https://doi.org/10.3969/j.issn.1001-1528.2024.06.044.
115 Fang H, Gao BB, Zhao YL, et al. Curdione inhibits thrombin-induced platelet aggregation *via* regulating the AMP-activated protein kinase-vinculin/talin-integrin αIIbβ3 sign pathway. *Phytomedicine*. 2019;61:152859. https://doi.org/10.1016/j.phymed.2019.152859.
116 Kaplangoray M, Toprak K, Cekici Y, et al. Relationship between blood viscosity and thrombus burden in ST-segment elevation myocardial infarction. *Clin Hemorheol Microcirc*. 2023;85(1):31-40. https://doi.org/10.3233/CH-231756.
117 Çınar T, Şaylık F, Akbulut T, et al. The association between whole blood viscosity and high thrombus burden in patients with non-ST elevation myocardial infarction. *Kardiol Pol*. 2022;80(4):429-435. https://doi.org/10.33963/KP.a2022.0043.
118 Receveur N, Nechipurenko D, Knapp Y, et al. Shear rate gradients promote a bi-phasic thrombus formation on weak adhesive proteins, such as fibrinogen in a VWF-dependent manner. *Haematologica*. 2020;105(10): 2471-2483. https://doi.org/10.3324/haematol.2019.235754.
119 Casa LDC, Ku DN. Thrombus formation at high shear rates. *Annu Rev Biomed Eng*. 2017;19:415-433. https://doi.org/10.1146/annurev-bioeng-071516-044539.
120 Si L, Wang X, Chen XH, et al. Effect of curdione on hemorheological indexs in rats with blood stasis syndrome. *Anhui Med and Pharm J*. 2012;16(09): 1229-1231.
121 Tan C, Jin Y, Xia Q. Experimental study of the anti-inflammatory and analgesic of curdione. *Chin J Bone Tumor Bone Dis*. 2009;8(3):168-170. https://doi.org/10.3969/j.issn.1671-1971.2009.06.011.
122 Shi H, Shi L, Li JX. Effects of curdione on cognitive function and expression of inflammatory factors in the hippocampus after partial hepatectomy in aged mice. *J Xi'an Jiaotong Univ Med Sci*. 2017;38(5):749-752. https://doi.org/10.7652/jdyxb201705026.
123 Echizen K, Hirose O, Maeda Y, et al. Inflammation in gastric cancer: Interplay of the COX-2/prostaglandin E2 and Toll-like receptor/MyD88 pathways. *Cancer Sci*. 2016;107(4):391-397. https://doi.org/10.1111/cas.12901.
124 Nasry W, Rodriguez-Lecompte J, Martin C. Role of COX-2/PGE2 mediated inflammation in oral squamous cell carcinoma. *Cancers*. 2018;10(10):348. https://doi.org/10.3390/cancers10100348.
125 Oh OJ, Min HY, Lee SK. Inhibition of inducible prostaglandin E2 production and cyclooxygenase-2 expression by curdione from *Curcuma zedoaria*. *Arch Pharm Res*. 2007;30(10):1236-1239. https://doi.org/10.1007/BF02980264.
126 Shi YY, Luo P, Wang WK, et al. M1 but not M0 extracellular vesicles induce polarization of RAW264.7 macrophages *via* the TLR4-NF-κB pathway in vitro. *Inflammation*. 2020;43(5):1611-1619. https://doi.org/10.1007/s10753-020-01236-7.
127 Cai YJ, Qiu L, Tao XY. *Study on the effect of curdione in alleviating colitis in mice*. In: The 6th International Scientific Conference on Probiotics and Prebiotics. IPC. 2024;87. https://doi.org/10.26914/c.cnkihy.2024.079038.
128 Wu ZM, Zai WJ, Chen W, et al. Curdione ameliorated doxorubicin-induced cardiotoxicity through suppressing oxidative stress and activating Nrf2/HO-1 pathway. *J Cardiovasc Pharmacol*. 2019;74(2):118-127. https://doi.org/10.1097/FJC.0000000000000692.
129 Ma YL, Wang PH, Wu ZM, et al. Curdione relieved isoproterenol-induced myocardial damage through inhibiting oxidative stress and apoptosis. *Am J Chin Med*. 2023;51(1):73-89. https://doi.org/10.1142/S0192415X23500052.
130 Ho HY, Cheng ML, Chen CM, et al. Oxidative damage markers and antioxidants in patients with acute myocardial infarction and their clinical significance. *BioFactors*. 2008;34(2):135-145. https://doi.org/10.1002/biof.5520340205.
131 Lillo-Moya J, Rojas-Solé C, Muñoz-Salamanca D, et al. Targeting ferroptosis against ischemia/reperfusion cardiac injury. *Antioxidants*. 2021;10(5):667. https://doi.org/10.3390/antiox10050667.
132 Wang HH, Xie B, Shi ST, et al. Curdione inhibits ferroptosis in isoprenaline-induced myocardial infarction *via* regulating Keap1/Trx1/GPX4 signaling pathway. *Phytother Res*. 2023;37(11):5328-5340. https://doi.org/10.1002/ptr.7964.
133 Rathore P, Dohare P, Varma S, et al. *Curcuma* oil: reduces early accumulation of oxidative product and is anti-apoptogenic in transient focal ischemia in rat brain. *Neurochem Res*. 2008;33(9):1672-1682. https://doi.org/10.1007/s11064-007-9515-6.
134 Prakash P, Misra A, Surin W, et al. Anti-platelet effects of *Curcuma* oil in experimental models of myocardial ischemia-reperfusion and thrombosis. *Thromb Res*. 2011;127(2):111-118. https://doi.org/10.1016/j.thromres.2010.11.007.
135 Manhas A, Khanna V, Prakash P, et al. Curcuma oil reduces endothelial cell-mediated inflammation in postmyocardial ischemia/reperfusion in rats. *J Cardiovasc Pharmacol*. 2014;64(3):228-236. https://doi.org/10.1097/FJC.0000000000000110.
136 Li XJ, Liang L, Shi HX, et al. Neuroprotective effects of curdione against focal cerebral ischemia reperfusion injury in rats. *Neuropsychiatr Dis Treat*. 2017;13:1733-1740. https://doi.org/10.2147/NDT.S139362.
137 Gauldie J, Bonniaud P, Sime P, et al. TGF-β, Smad3 and the process of progressive fibrosis. *Biochem Soc Trans*. 2007;35:661-664. https://doi.org/10.1042/BST0350661.
138 Gauldie J, Kolb M, Ask K, et al. Smad3 signaling involved in pulmonary fibrosis and emphysema. *Biochem Soc Trans*. 2006;3(8):696-702. https://doi.org/10.1513/pats.200605-125SF.
139 Bonniaud P, Margetts P, Ask K, et al. TGF-β and Smad3 signaling link inflammation to chronic fibrogenesis. *J Immunol*. 2005;175(8):5390-5395. https://doi.org/10.4049/jimmunol.175.8.5390.
140 Liu P, Miao K, Zhang L, et al. Curdione ameliorates bleomycin-induced pulmonary fibrosis by repressing TGF-β-induced fibroblast to myofibroblast differentiation. *Respir Res*. 2020;21(1):58. https://doi.org/10.1186/s12931-020-1300-y.
141 Zou SJ, Jie HY, Han XA, et al. The role of neutrophil extracellular traps in sepsis and sepsis-related acute lung injury. *Int Immunopharmacol*. 2023;124(Pt A):110436. https://doi.org/10.1016/j.intimp.2023.110436.
142 Zhang H, Liu JL, Zhou YL, et al. Neutrophil extracellular traps mediate m(6)A modification and regulates sepsis-associated acute lung injury by activating ferroptosis in alveolar epithelial cells. *Int J Biol Sci*. 2022;18(8): 3337-3357. https://doi.org/10.7150/ijbs.69141.
143 Qu MD, Chen ZY, Qiu ZY, et al. Neutrophil extracellular traps-triggered impaired autophagic flux *via* METTL3 underlies sepsis-associated acute lung injury. *Cell Death Discov*. 2022;8(1):375. https://doi.org/10.1038/s41420-022-01166-3.
144 Yang K, Wu B, Wei W, et al. Curdione ameliorates sepsis-induced lung injury by inhibiting platelet-mediated neutrophil extracellular trap formation. *Int Immunopharmacol*. 2023;118:110082. https://doi.org/10.1016/j.intimp.2023.110082.
145 Liu YN, Liu ZT, Wang KW. The Ca^{2+}-activated chloride channel ANO1/TMEM16A: an emerging therapeutic target for epithelium-originated diseases? *Acta Pharm Sin B*. 2021;11(6):1412-1433. https://doi.org/10.1016/j.apsb.2020.12.003.
146 Grigoriev VV. Calcium-activated chloride channels: structure, properties, role in physiological and pathological processes. *Biomed Khim*. 2021;67(1): 17-33. https://doi.org/10.18097/pbmc20216701017.
147 Yang YD, Cho HW, Koo JY, et al. TMEM16A confers receptor-activated calcium-dependent chloride conductance. *Nature*. 2008;455(7217):1210-1215. https://doi.org/10.1038/nature07313.
148 Terashima H, Picollo A, Accardi A. Purified TMEM16A is sufficient to form Ca^{2+}-activated Cl- channels. *Proc Natl Acad Sci USA*. 2013;110(48):19354-19359. https://doi.org/10.1073/pnas.1312014110.
149 Huang F, Zhang HK, Wu M, et al. Calcium-activated chloride channel TMEM16A modulates mucin secretion and airway smooth muscle contraction. *Proc Natl Acad Sci USA*. 2012;109(40):16354-16359. https://doi.org/10.1073/pnas.1214596109.
150 Cabrita I, Benedetto R, Wanitchakool P, et al. TMEM16A mediates mucus production in human airway epithelial cells. *Proc Natl Acad Sci USA*. 2021; 64(1):50-58. https://doi.org/10.1165/rcmb.2019-0442OC.
151 Benedetto R, Cabrita I, Schreiber R, et al. TMEM16A is indispensable for

basal mucus secretion in airways and intestine. *FASEB J*. 2019;33(3):4502-4512. https://doi.org/10.1096/fj.201801333RRR.
152 Zhu XJ, Zhang WT, Jin LL, et al. Inhibitory activities of curzerenone, curdione, furanodienone, curcumol and germacrone on Ca-activated chloride channels. *Fitoterapia*. 2020;147:104736. https://doi.org/10.1016/j.fitote.2020.104736.
153 Matsuda H, Ninomiya K, Morikawa T, et al. Inhibitory effect and action mechanism of sesquiterpenes from Zedoariae Rhizoma on D-galactosamine /lipopolysaccharide-induced liver injury. *Bioorg Med Chem Lett*. 1998;8(4):339-344. https://doi.org/10.1016/S0960-894X(98)00021-3.
154 Morikawa T, Matsuda H, Ninomiya K, et al. Medicinal foodstuffs. XXIX. Potent protective effects of sesquiterpenes and curcumin from Zedoariae Rhizoma on liver injury induced by D-galactosamine/lipopolysaccharide or tumor necrosis factor-alpha. *Bioorg Med Chem Lett*. 2002;25(5):627-631. https://doi.org/10.1248/bpb.25.627.
155 Tsuchida T, Friedman SL. Mechanisms of hepatic stellate cell activation. *Nat Rev Gastroenterol Hepatol*. 2017;14(7):397-411. https://doi.org/10.1038/nrgastro.2017.38.
156 Thoen L, Guimarães E, Dollé L, et al. A role for autophagy during hepatic stellate cell activation. *J Hepatol*. 2011;55(6):1353-1360. https://doi.org/10.1016/j.jhep.2011.07.010.
157 Zhou YN, Long D, Zhao Y, et al. Oxidative stress-mediated mitochondrial fission promotes hepatic stellate cell activation *via* stimulating oxidative phosphorylation. *Cell Death Dis*. 2022;13(8):689. https://doi.org/10.1038/s41419-022-05088-x.
158 Bates J, Vijayakumar A, Ghoshal S, et al. Acetyl-CoA carboxylase inhibition disrupts metabolic reprogramming during hepatic stellate cell activation. *J Hepatol*. 2020;73(4):896-905. https://doi.org/10.1016/j.jhep.2020.04.037.
159 Hao M, Yao ZH, Zhao MT, et al. Active ingredients screening and pharmacological mechanism research of curcumae rhizoma-sparganii rhizoma herb pair ameliorates liver fibrosis based on network pharmacology. *J Ethnopharmacol*. 2023;305:116111. https://doi.org/10.1016/j.jep.2022.116111.
160 Dai WZ, Qin Q, Li ZY, et al. Curdione and schisandrin C synergistically reverse Hepatic fibrosis *via* modulating the TGF-β pathway and inhibiting oxidative stress. *Front Cell Dev Biol*. 2021;9:763864. https://doi.org/10.3389/fcell.2021.763864.
161 Ling L, Qing X, Gang B, et al. Anti-H1N1 viral activity of three main active ingredients from zedoary oil. *Fitoterapia*. 2020;142:104489. https://doi.org/10.1016/j.fitote.2020.104489.
162 Quesada-Ocampo L, Parada-Rojas C, Hansen Z, et al. Phytophthora capsici: recent progress on fundamental biology and disease management 100 years after Its description. *Annu Rev Phytopathol*. 2023;61:185-208. https://doi.org/10.1146/annurev-phyto-021622-103801.
163 Niu G, Yang Q, Liao Y, et al. Advances in understanding Fusarium graminearum: genes involved in the regulation of sexual development, pathogenesis, and deoxynivalenol biosynthesis. *Genes*. 2024;15(4):475. https://doi.org/10.3390/genes15040475.
164 Khan M, Pandey A, Athar T, et al. Fusarium head blight in wheat: contemporary status and molecular approaches. *3 Biotech*. 2020;10(4):172. https://doi.org/10.1007/s13205-020-2158-x.
165 Chen CQ, Long LI, Zhang FS, et al. Antifungal activity, main active components and mechanism of *Curcuma longa* extract against *Fusarium graminearum*. *PLoS One*. 2018;13(3):e0194284. https://doi.org/10.1371/journal.pone.0194284.
166 Mushtaq A, Azam U, Mehreen S, et al. Synthetic *α*-glucosidase inhibitors as promising anti-diabetic agents: recent developments and future challenges. *Eur J Med Chem*. 2023;249:115119. https://doi.org/10.1016/j.ejmech.2023.115119.
167 Cai Y, Xie H, Zhang J, et al. An updated overview of synthetic *α*-glucosidase inhibitors: chemistry and bioactivities. *Curr Top Med Chem*. 2023;23(26):2488-2526. https://doi.org/10.2174/1115680266260682230921054652.
168 Hossain U, Das AK, Ghosh S, et al. An overview on the role of bioactive *α*-glucosidase inhibitors in ameliorating diabetic complications. *Food Chem Toxicol*. 2020;145:111738. https://doi.org/10.1016/j.fct.2020.111738.
169 Joshi SR, Standl E, Tong NW, et al. Therapeutic potential of *α*-glucosidase inhibitors in type 2 diabetes mellitus: an evidence-based review. *Expert Opin Pharmacother*. 2015;16(13):1959-1981. https://doi.org/10.1517/14656566.2015.1070827.
170 Zhou CX, Zhang LS, Chen FF, et al. Terpenoids from *Curcuma wenyujin* increased glucose consumption on HepG2 cells. *Fitoterapia*. 2017;121:141-145. https://doi.org/10.1016/j.fitote.2017.06.011.
171 Ain Ibrahim N, Kamal N, Mediani A, et al. ^{1}H NMR-based metabolomics approach revealing metabolite variation of black turmeric (*Curcuma caesia*) extracts and correlation with its antioxidant and *α*-glucosidase inhibitory activities. *Food Technol Biotechnol*. 2023;61(1):107-117. https://doi.org/10.17113/ftb.61.01.23.7711.
172 Shaw R, Cantley L. Ras, PI(3)K and mTOR signalling controls tumour cell growth. *Nature*. 2006;441(7092):424-430. https://doi.org/10.1038/nature04869.
173 Hay N, Sonenberg N. Upstream and downstream of mTOR. *Genes Dev*. 2004;18(16):1926-1945. https://doi.org/10.1101/gad.1212704.
174 Bai XZ, He T, Liu JQ, et al. Loureirin B inhibits fibroblast proliferation and extracellular matrix deposition in hypertrophic scar *via* TGF-β/Smad pathway. *Exp Dermatol*. 2015;24(5):355-360. https://doi.org/10.1111/exd.12665.
175 Song BY, Zhu YH, Zhao Y, et al. Machine learning and single-cell transcriptome profiling reveal regulation of fibroblast activation through THBS2/TGFβ1/P-Smad2/3 signalling pathway in hypertrophic scar. *Int Wound J*. 2024;21(3):e14481. https://doi.org/10.1111/iwj.14481.
176 Zhang H, Lin C, Zhou JM, et al. Pharmacological analysis of curdione on hypertrophic scar fibroblast. *Chin Tradit Herbal Drugs*. 2018;49(8):1854-1859. https://doi.org/10.7501/j.issn.0253-2670.2018.08.018.
177 Meng X, Zhang T, Li Y, et al. The toxicokinetic profile of curdione in pregnant SD rats and its transference in a placental barrier system detected by LC-MS/MS. *Regul Toxicol Pharmacol*. 2015;71(2):158-163. https://doi.org/10.1016/j.yrtph.2014.12.005.
178 Wu QB, Chen MT, Lin YF, et al. Multiomics profiling uncovers curdione-induced reproductive toxicity in HTR-8/SVneo cells. *Heliyon*. 2024;10(21):e38650. https://doi.org/10.1016/j.heliyon.2024.e38650.
179 Fonseca W, Monteiro C, Taborda-Barata L. Inhaled drug therapy-associated adverse reactions in obstructive respiratory diseases: a review of a decade of reporting to the portuguese pharmacovigilance system. *Int J Environ Res Public Health*. 2021;18(23):12411. https://doi.org/10.3390/ijerph182312411.
180 Kalyanasundaram A, Lincoff A. Managing adverse effects and drug-drug interactions of antiplatelet agents. *Nat Rev Cardiol*. 2011;8(10):592-600. https://doi.org/10.1038/nrcardio.2011.128.
181 Long K, Suresh K. Pulmonary toxicity of systemic lung cancer therapy. *Respirology*. 2020;25(2):72-79. https://doi.org/10.1111/resp.13915.
182 Chang H, Wu SF, Li YJ, et al. Analysis of 737 reports of adverse drug reactions induced by Zedoray Turmeric Oil Injection and literature review. *Chin J Pharmacovigilance*. 2017;14(6):359-363.
183 Yang ZR, Wang ZZ, Li JL, et al. Network pharmacology-based dissection of the underlying mechanisms of dyspnoea induced by zedoary turmeric oil. *Basic Clin Pharmacol Toxicol*. 2022;130(5):606-617. https://doi.org/10.1111/bcpt.13722.
184 Niu J, Straubinger RM, Mager DE. Pharmacodynamic drug-drug interactions. *Clin Pharmacol Ther*. 2019;105(6):1395-1406. https://doi.org/10.1002/cpt.1434.
185 Mar P, Horbal P, Chung M, et al. Drug interactions affecting antiarrhythmic drug use. *Circ Arrhythm Electrophysiol*. 2022;15(5):e007955. https://doi.org/10.1161/CIRCEP.121.007955.
186 Wang M, Zeraatkar D, Obeda M, et al. Drug-drug interactions with warfarin: a systematic review and meta-analysis. *Br J Clin Pharmacol*. 2021;87(11):4051-4100. https://doi.org/10.1111/bcp.14833.
187 Lynch T, Price A. The effect of cytochrome P450 metabolism on drug response, interactions, and adverse effects. *Am Fam Physician*. 2007;76(3):391-396. https://doi.org/10.1365/s10337-004-0469-4.
188 Hakkola J, Hukkanen J, Turpeinen M, et al. Inhibition and induction of CYP enzymes in humans: an update. *Arch Toxicol*. 2020;94(11):3671-3722. https://doi.org/10.1007/s00204-020-02936-7.
189 Tian DD, Hu ZY. CYP3A4-mediated pharmacokinetic interactions in cancer therapy. *Curr Drug Metab*. 2014;15(8):808-817. https://doi.org/10.2174/1389200216666150223152627.
190 Hou XL, Hayashi-Nakamura E, Takatani-Nakase T, et al. Curdione plays an important role in the inhibitory effect of *Curcuma aromatica* on CYP3A4 in Caco-2 cells. *Evid Based Compl Alt*. 2011;2011:913898. https://doi.org/10.1093/ecam/nep229.
191 Wei WL, Li ZW, Li Hj, et al. The inhibitory effect of 225 frequently-used traditional Chinese medicines for CYP3A4 metabolic enzyme by isoform-specific probe. *Fitoterapia*. 2021;152:104858. https://doi.org/10.1016/j.fitote.2021.104858.
192 Liu SY, Zhao Y, Tang X, et al. *In vitro* inhibition of six active sesquiterpenoids in zedoary turmeric oil on human liver cytochrome P450 enzymes. *J Ethnopharmacol*. 2024;322:117588. https://doi.org/10.1016/j.jep.2023.117588.